

AWARD NUMBER: W81XWH-18-1-0561

TITLE: NOXA Loss as a Major Mechanism of Intrinsic Resistance to Targeted Therapies in Breast Cancer

PRINCIPAL INVESTIGATOR: Anthony Faber PH.D.

CONTRACTING ORGANIZATION: Virginia Commonwealth University, Richmond, VA

REPORT DATE: January 2023

TYPE OF REPORT: FINAL

PREPARED FOR: U.S. Army Medical Research and Development Command
Fort Detrick, Maryland 21702-5012

DISTRIBUTION STATEMENT: Approved for Public Release;
Distribution Unlimited

The views, opinions and/or findings contained in this report are those of the author(s) and should not be construed as an official Department of the Army position, policy or decision unless so designated by other documentation.

REPORT DOCUMENTATION PAGE

Form Approved
OMB No. 0704-0188

Public reporting burden for this collection of information is estimated to average 1 hour per response, including the time for reviewing instructions, searching existing data sources, gathering and maintaining the data needed, and completing and reviewing this collection of information. Send comments regarding this burden estimate or any other aspect of this collection of information, including suggestions for reducing this burden to Department of Defense, Washington Headquarters Services, Directorate for Information Operations and Reports (0704-0188), 1215 Jefferson Davis Highway, Suite 1204, Arlington, VA 22202-4302. Respondents should be aware that notwithstanding any other provision of law, no person shall be subject to any penalty for failing to comply with a collection of information if it does not display a currently valid OMB control number. **PLEASE DO NOT RETURN YOUR FORM TO THE ABOVE ADDRESS.**

1. REPORT DATE January 2023		2. REPORT TYPE Final		3. DATES COVERED 30Sep2018-29Sep2022	
4. TITLE AND SUBTITLE NOXA Loss as a Major Mechanism of Intrinsic Resistance to Targeted Therapies in Breast Cancer				5a. CONTRACT NUMBER	
				5b. GRANT NUMBER W81XWH-18-1-0561	
				5c. PROGRAM ELEMENT NUMBER	
6. AUTHOR(S) Anthony Faber, Jorge S Reis-Filho Email: acfaber@vcu.edu; reisfilj@mskcc.org				5d. PROJECT NUMBER	
				5e. TASK NUMBER	
				5f. WORK UNIT NUMBER	
7. PERFORMING ORGANIZATION NAME(S) AND ADDRESS(ES) Site 1: Virginia Commonwealth University, 907 Floyd Avenue, Richmond, VA 23284 Site 2: Memorial Sloan Kettering Cancer Center 1275 York Avenue New York, NY				8. PERFORMING ORGANIZATION REPORT NUMBER	
9. SPONSORING / MONITORING AGENCY NAME(S) AND ADDRESS(ES) U.S. Army Medical Research and Development Command Fort Detrick, Maryland 21702-5012				10. SPONSOR/MONITOR'S ACRONYM(S)	
				11. SPONSOR/MONITOR'S REPORT NUMBER(S)	
12. DISTRIBUTION / AVAILABILITY STATEMENT Approved for Public Release; Distribution Unlimited					
13. SUPPLEMENTARY NOTES					
14. ABSTRACT Our grant hypothesis was that MCL-1 inhibition can sensitize HER2 inhibitors in HER2 amplified breast cancer and ER inhibitors in ER-positive breast cancer. We have provided preclinical evidence to support the use to ER inhibitors in combination with MCL-1 inhibitors in ER+ breast cancer and our findings have uncovered a novel axis of miRNA4728-NOXA-MCL-1 as a key determinant of sensitivity of HER2 inhibitors in HER2 amplified breast cancers and ER inhibitors in ER+ breast cancers. In addition, HER2 inhibitor treatment and ER inhibitor treatment both lead to loss of NOXA, which causes a MCL-1 addiction. In this sensitivity. NOXA-high and MCL1-low ER-positive/HER2-negative breast cancers were associated with shorter recurrence free survival. Given these findings and given the success of anti-HER2 antibody drug conjugates in HER2- <i>amplified</i> (HER2- positive) breast cancer, during the past 12 months we have deprioritized HER2-positive disease and focused on ER- positive/HER2-negative breast cancers, expanding our analyses to additional ER-positive/HER2-negative breast cancer cohorts. Through IHC and omics studies, we have a higher extent of tumor infiltrating lymphocytes and a higher tumor mutational burden in NOXA-high and MCL-1-high ER-positive/HER2-negative breast cancers, as well as an enrichment in pathogenic genetic alterations affecting the <i>WHSC1L1</i> , <i>BAP1</i> and <i>PRKAR1A</i> in NOXA-high ER-positive/HER2- negative breast cancer samples as compared to NOXA-low samples. We are preparing a second manuscript from this project, titled ER-positive/HER2-negative breast cancer and the NOXA/MCL1 axis: A genomic characterization.					
15. SUBJECT TERMS MCL1, targeted therapy, apoptosis, resistance, NOXA					
16. SECURITY CLASSIFICATION OF:			17. LIMITATION OF ABSTRACT	18. NUMBER OF PAGES	19a. NAME OF RESPONSIBLE PERSON
a. REPORT	b. ABSTRACT	c. THIS PAGE			USAMRMC
Unclassified	Unclassified	Unclassified	Unclassified	32	19b. TELEPHONE NUMBER (include area code)

TABLE OF CONTENTS

Page

1. Introduction	p.4
2. Keywords	p.4
3. Accomplishments	p.4-15
4. Impact	p.16
5. Changes/Problems	p.16
6. Products	p.16
7. Participants & Other Collaborating Organizations	p.16
8. Special Reporting Requirements	p.17

1. Introduction

HER2-amplified breast cancers and Estrogen receptor (ER) positive breast cancers are susceptible to *HER2* inhibitors and ER inhibitors, respectively. However, treatment with these targeted agents elicit transient responses, and ways to sensitize these cancers further with the addition of rationally implemented targeted therapies continues to be the subject of intense research. In this grant, we have posited that low expression of the endogenous MCL-1 inhibitor, NOXA, in *HER2*-amplified breast cancers causes 1) resistance to *HER2* inhibitors through MCL-1 activity and 2) susceptible to combination therapy with MCL-1 inhibitors. The mechanism is through suppression of ER-mediated loss of NOXA transcription, which is mediated by miRNA4728, a coamplified gene with *HER2* in these cancers. In addition, by way of a overlapping mechanism, in ER+ breast cancers, treatment with ER inhibitors leads to loss of NOXA transcription. In both cases, addition of MCL-1 inhibitors – either MCL-1 BH3 mimetics or CDK inhibitors that block MCL-1 transcription – can induce cell death.

2. Keywords: *MCL1*, targeted therapy, apoptosis, resistance, NOXA, *HER2*, breast cancer

3. Accomplishments

Major Task 1

Characterize the miRNA4728/ER/NOXA axis in *HER2*-amplified breast cancers and its role in intrinsic resistance to *HER2*i

Subtask 1: In collaboration with Dr. Mikhail Dozmorov (VCU), we will analyze annotated breast cancer samples in CCLE and other publically-available databases to determine if NOXA and/or MCL-1 levels predict responses and survival in breast cancer

We first evaluated NOXA (encoded by *PMAIP1*) and MCL1 RNA levels from TCGA. Briefly, open access gene expression data summarized as RSEM values were obtained using the TCGA2STAT R package v 1.2, along with the corresponding clinical annotations. Briefly, open access gene expression data summarized as RSEM values were obtained using the TCGA2STAT R package v 1.2, along with the corresponding clinical annotations.

To determine if NOXA and/or MCL-1 levels predict responses and survival in breast cancer, we analyzed annotated breast cancer samples in publicly available cancer genomics databases.

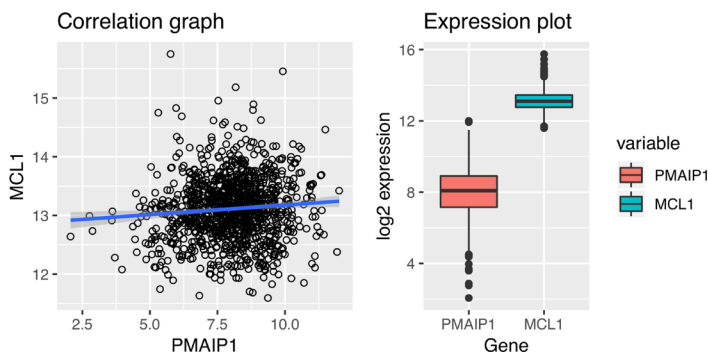


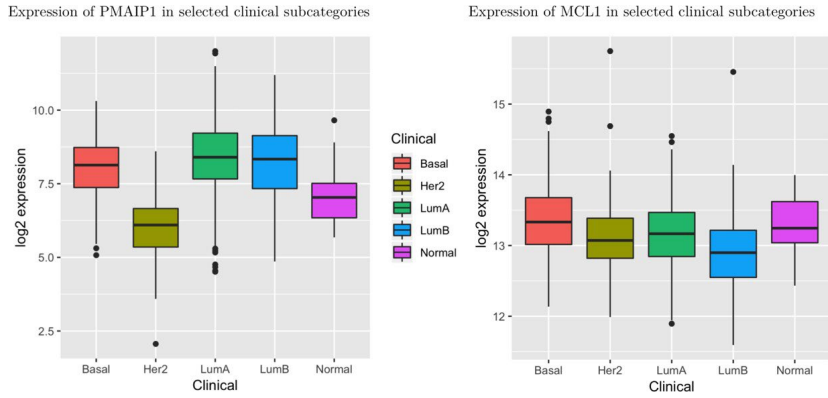
Figure 1. MCL1 is highly expressed in breast cancer and uncorrelated with NOXA RNA expression.

Within all breast cancer samples in the TCGA, NOXA was expressed at a lower level than MCL1 (Fig. 1). However, the expression of NOXA and MCL1 RNA were poorly correlated (Pearson correlation 0.038, p-value = 0.231), as would be expected since NOXA inhibits MCL-1 protein expression, and not MCL1 RNA.

We evaluated the effect of NOXA and MCL1 expression on overall survival. Briefly, the data was log2-transformed and analyzed using Kaplan-Meier curves and Cox proportional hazard model. A modified approach was

used to estimate the best gene expression cutoff that separates high/low expression subgroups with differential survival.

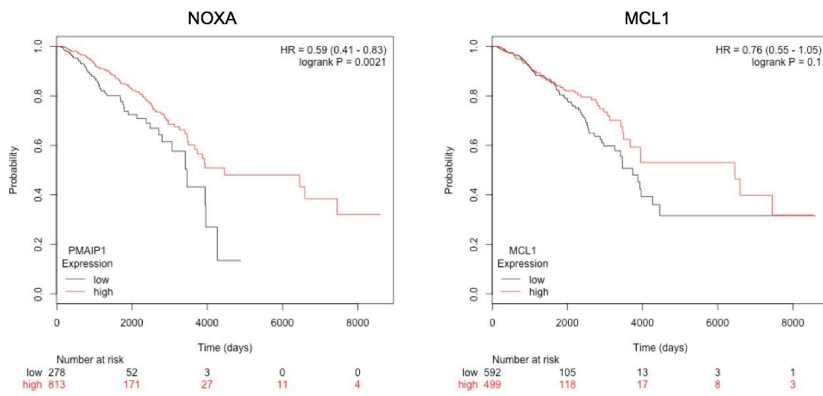
We classified breast cancer samples using the gold-standard PAM50 classifier into five subtypes (Normal-like, Basal, HER2 amplified (Her2), luminal A (LumA), and luminal B (LumB)). The expression of both NOXA and MCL1 was significantly different across the subtypes (ANOVA p-value < 2.2e-16 and 3.82e-13 for NOXA and MCL1, respectively).



Tukey's honest significance difference (HSD) test identified NOXA expression as significantly lower in the Her2 subtype as compared with LumA, LumB, and Basal subtypes (Tukey's HSD p-value = 3.164e-13, 3.165e-13, and 3.637e-13, respectively,

Figure 2). The expression differences were less pronounced for MCL1, where its expression in the HER2 amplified subtype was significantly higher than in LumB subtype (Tukey's HSD p-value = 0.001759). **These results demonstrate the overall low expression of NOXA in HER2 amplified breast cancer, consistent with our hypothesis.**

Figure 2. High NOXA and MCL1 are positively associated with survival in breast cancer.



High expression of both NOXA and MCL1 were associated with better survival in breast cancer (Figure 3). Yet, this effect was significant only for NOXA (log-rank p-value = 0.0021). These data likely reflect the better survival rates in ER+ breast cancer compared to other subtypes.

Figure 3. High NOXA and MCL1 are positively associated with survival in breast cancer.

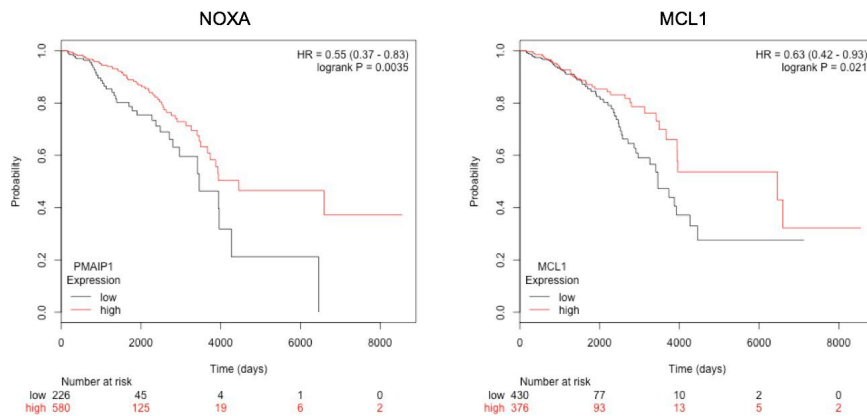


Figure 4. Estrogen receptor-positive breast cancer samples are the most associated with NOXA and MCL1 expression.

To further investigate the survival effect of NOXA and MCL1, we took advantage of the availability of clinical annotations. We performed survival analysis on subsets of patients annotated with specific clinical annotations were selected (e.g., “PAM50Call_RNAseq-LumA” or “radiation_therapy-NO” clinical annotations). Subgroups with < 40 patients were not considered.

ER+ breast cancers were among the most susceptible to NOXA and MCL1 gene expression changes (Figure 4). Similar to the survival effect in all breast cancer samples, higher expression of either NOXA or MCL1 was associated with improved survival, and this effect was the most significant in NOXA (p-value = 0.0035). These data imply that ER+ breast cancers with high activity of ER (as NOXA is a direct target) may be the most treatable. Our expectation is higher MCL1 levels would predict poorer response. As

MCL1 is highly regulated at the post-translational level, these data suggest to us the analyses of MCL1 protein levels by IHC will be important to determine whether MCL1 levels predict survival.

We extended our data analyses to a dataset of ER+ breast cancer patients on the ER inhibitor, Letrozole. Pretreatment and Letrozole breast tumors were assessed over 2 weeks in a publically available database. Interestingly, we found that the NOXA mRNA levels were markedly suppressed following 2 weeks of letrozole treatment compared to the mRNA levels of the other BCL2 family members (BBC3: PUMA, BCL2L11: BIM, BCL2L1: BCL-XL) (Figure 5). This result of other BCL-2 members not changing supports our previous observation of low expression of NOXA in HER2 amplified breast cancer as the

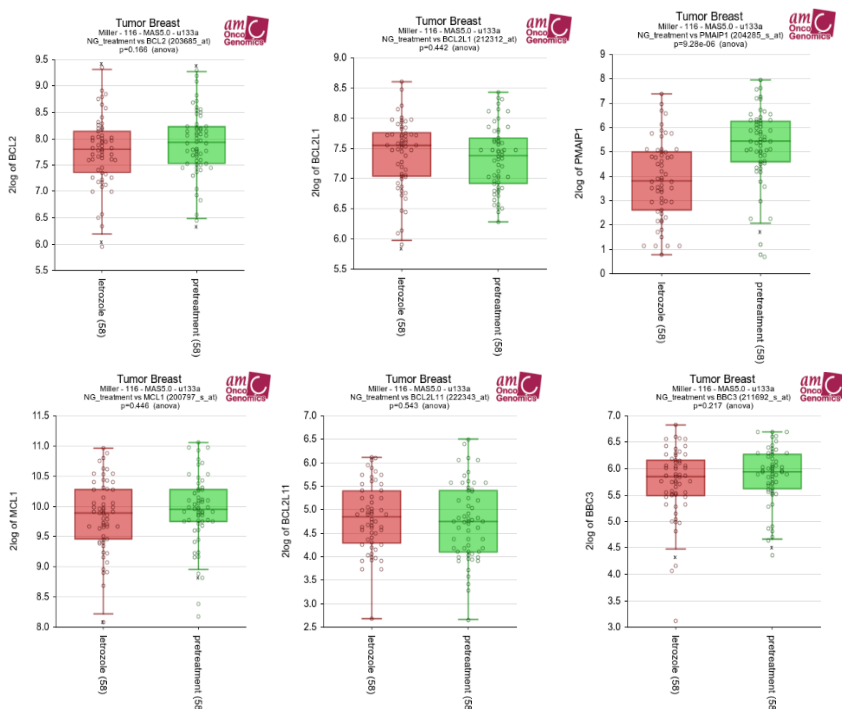


Figure 5. Changes in BCL-2 members over 2 weeks from Letrozole treatment. Of note, no significant changes except NOXA is markedly lower in the post-letrozole treatments.

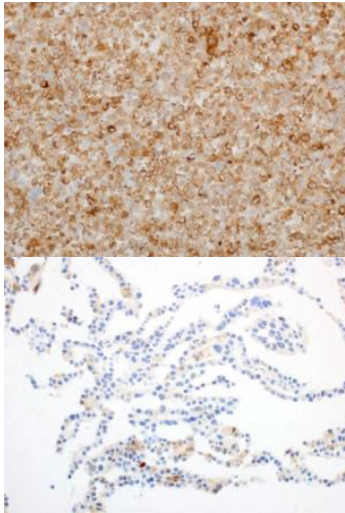
important alteration following ER inhibition, and is consistent with that of our hypothesis.

TISSUE	Diagnosis	IHC Result (prelim)
MDA-MB453 NOXA OE; cell pellet	NOXA negative control	+ cp/ncl
SKBR3 NOXA OE; cell pellet	SKBR3 (NOXA (transf/overexpression))	++++ cp,w
SKnDZ NOXA KD; cell pellet	SKnDZ NOXA-knock-down	neg (foc)
EFM192A EV; cell pellet	NOXA negative control	++ cp
SKBR3 EV; cell pellet	SKBR3 (empty vector)	+++ cp
EFM192A NOXA OE; cell pellet	NOXA negative control	++++ cp granular
SK-N-BE2 EV; cell pellet	SK-N-BE2 (empty vector)	foc cp w

Table 1.

Subtask 2: In collaboration with Dr. Edi Brogi, (Director of Breast Pathology, MSKCC), and Dr. Mikhail Dozmorov (Department of Biostatistics, VCU), we will evaluate 180 samples of clinically annotated HER2+ breast cancer specimens collected at MSKCC for HER2 levels, NOXA levels, and MCL-1 levels by immunohistochemistry.

Image 1. Validation of NOXA AB 114C307. (Top) staining of cell line H1048 (high NOXA expression, 20x). (below) staining of cell line EFM-192A (low NOXA)



We have gone through the process of validation by using a series of molecularly altered cell lines including syngenic lines with manipulation of NOXA in breast cancer cell lines (Table 1 cell lines and results of staining, OE=overexpression, KD=knockdown).

Immunohistochemical Detection of NOXA/PMAIP1

In order to establish a rigorous assay for NOXA expression, Dr. Achim Jungbluth and Dr. Edi Brogi comprehensively evaluated NOXA/PMAIP1 commercial reagents. Due to the inherent inconsistency of polyclonal reagents, the search for suitable reagents was focused on monoclonal antibodies. All immunohistochemical stains were performed on a Leica Bond-3 (Leica, Buffalo Grove, IL) automated stainer platform and on formalin-fixed paraffin embedded tissues. Initial testing of clones was done on a panel of ten normal tissues. Optimization assays comprised of modifying titration steps as well as heat-based antigen retrieval steps using low pH citrate (ER1, Leica) and hipH TRIS buffer (ER2, Leica). A polymer based secondary kit (Refine, Leica) was used to detect the primary.

In the initial testing, clone D8L7U (#147665; Cell Signaling Technology, Danvers, MA) did not reveal any staining compatible with presence of NOXA/PMAIP1 (data not shown). Clone 114C307 (ab13654; Abcam, Cambridge, MA) showed staining in normal tissues compatible with expression of NOXA/PMAIP1. For example, strong staining was seen in tubules of the kidney cortex while testicular germ cells remained negative (data not shown). Specificity was further analyzed in formalin-fixed paraffin embedded pellets of various cell lines.

NOXA/PMAIP1 mRNA levels were tested by rt-PCR or compared to publicly available databases of the Broad Institute (<https://portals.broadinstitute.org/ccle>). Sample staining are shown in Image 1. We validated these findings in human neoplasms as well as known controls and the data are consistent with a robust assay that can score for NOXA expression with specificity and potential for quantitation. These robust controls have allowed us to validate confidently a NOXA antibody (ab13654). After testing different dilutions of the NOXA (mAb 114C307 - ab13654).

Immunohistochemical Detection of MCL-1

To establish a robust IHC assay for the assessment of MCL-1 expression, we assessed the performance of different commercially available antibodies against MCL-1. Based on the high and low MCL-1 mRNA expression levels of in MCF-7 (normalized protein-coding transcripts per million, nTPM=160.3) and HEK293 cells (nTPM)=68.3), respectively (PMID: 31857451), formalin-fixed paraffin embedded (FFPE) cell pellets were used as controls. As an orthogonal validation, we conducted the assessment of MCL-1 protein expression in HEK293 and MCF-7 cell lysates by western blot (MCL1 antibody, clone D2W9E; #94294, Cell Signaling Technology, Danvers, MA). In agreement with the gene expression levels, we observed higher MCL-1 protein levels in MCF7 cells compared to HEK293 cells (**Image 2A**). Using these FFPE cell pellets, as well as a panel of 10 normal tissues, we proceeded to assess the suitability of various monoclonal antibodies for the immunohistochemical detection of MCL-1, as well as their optimization, including the modification of titration steps. The MCL-1 (clone RC13) antibody (Santa Cruz Biotechnology, Dallas, Texas; dilution 1:100)

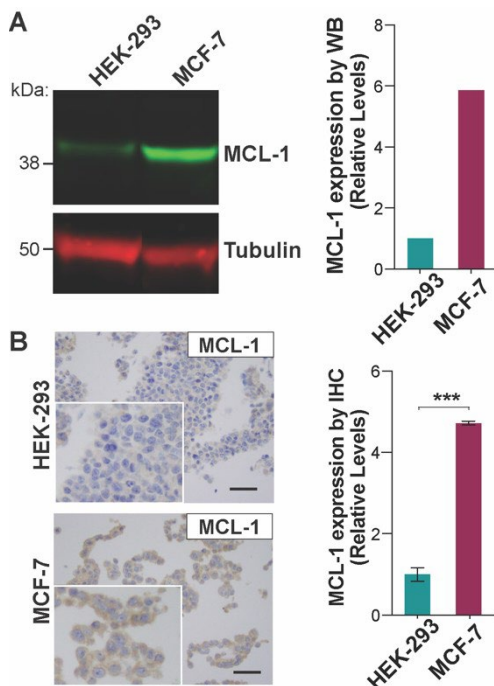


Image 2. Optimization of MCL-1 detection by immunohistochemistry. (A) MCL-1 protein expression in HEK-293 and MCF-7 cells by western blot and (B) MCL-1 protein expression by IHC using the clone RC13 MCL-1 antibody and the optimized protocol.

displayed expression in normal tissues compatible with the reported expression MCL-1 (PMID: 31857451), such as high expression in testis and low in lung (data not shown). Upon IHC analysis of the FFPE cell pellets with this clone, we observed statistically significantly higher MCL-1 protein expression levels in MCF-7 cells compared to HEK293 cells ($P=2.9 \times 10^{-5}$, student's t-test; **image 2B**), in agreement with our observations by western blot. Taken together, we have established a robust assay for detection of MCL-1 by IHC, which was used for the assessment in tissues samples.

Human Breast Cancer Sample Testing

We obtained HPRO approval and MSK IRB approval for our plans for testing breast cancers using this assay. We have further searched among an initial cohort of over 600 samples and unfortunately most of these were exhausted.

However, given the success and promise of Ado-trastuzumab emtansine (T-DM1) and trastuzumab deruxtecan (T-Dxd), the two FDA ADCs approved for HER2-positive breast cancer (PMID: 36255231, PMID: 35674041, PMID: 34380530, PMID: 34263665, PMID: 31825192, PMID: 31047803), along with the rapid development of novel and anti-HER2 ADCs, we have shifted the focus of this work towards the study of the ER/NOXA axis in ER- positive/HER2-negative breast cancer as detailed under **Major Task 2**.

Thus, we have employed the IHC assays we previously developed for assessment of MCL-1 and NOXA expression to focus on a cohort of ER-positive/HER2-negative breast cancers (**See below, Major Task 2**).

Subtask 3: In Dr. Scaltriti's laboratory, we will determine the role of NOXA/MCL-1 in a panel of HER2 amplified breast cancer intrinsic resistant models to diverse HER2 inhibitors

In the BT-474 cells (moderate HER2 inhibitor sensitivity) and MDA-MB-453 (intrinsically resistant to HER2 inhibitors) *HER2*-amplified breast cancer cells, we examined whether targeting MCL-1 would sensitize to diverse HER2 inhibitors. Indeed, using the MCL-1 inhibitor dinaciclib we saw robust sensitization to the HER2 inhibitor lapatinib (see Floros et al., appended, Fig. 1B and 1C). This sensitization was through on-target downregulation of MCL-1 (see Floros et al., appended, Fig. 1A) and subsequent apoptosis (see Floros et al., appended, Fig. 1D). Through immunoprecipitation studies, we demonstrate dinaciclib treatment leads to loss of BIM:MCL-1 complexes and BAK:MCL-1 complexes, leading to cell death (see Floros et al., appended, Fig. 1E). We noted similar sensitization of the MCL-1 inhibitors A1210477 or dinaciclib to lapatinib (see Floros et al., appended, Sup. Figs. 1 and 4).

To further probe the role of BAK:MCL-1 complexes, we knocked down BAK with shRNA and through a BAK Ab immunoprecipitation cell death assay in both the *HER2* amplified, HER2 inhibitor-intrinsic resistant HCC1419 and MDA-MB-453 breast cancer cells (see Floros et al., appended, Fig. 2A and 2B). We next overexpressed MCL-1 in the SKBR3 *HER2*-amplified breast cancer cells (*HER2* inhibitor sensitive) and intrinsic resistant cells (HCC1419) to determine if this would mitigate toxicity to *HER2* inhibitor treatment. Indeed, MCL-1 expression abrogated sensitivity to lapatinib (Floros et al., appended, Fig. 2C-2F).

We next repeated these experiments with the *HER2* inhibitor, Tucatinib. Again, we found MCL-1 was sufficient to induce intrinsic resistance, and, targeting MCL-1 with dinaciclib was sufficient to reverse intrinsic resistance (Floros et al., appended, Fig. 3). Again, dinaciclib did so by displacing BIM and BAK from MCL-1, echoing the mechanism of sensitivity to lapatinib.

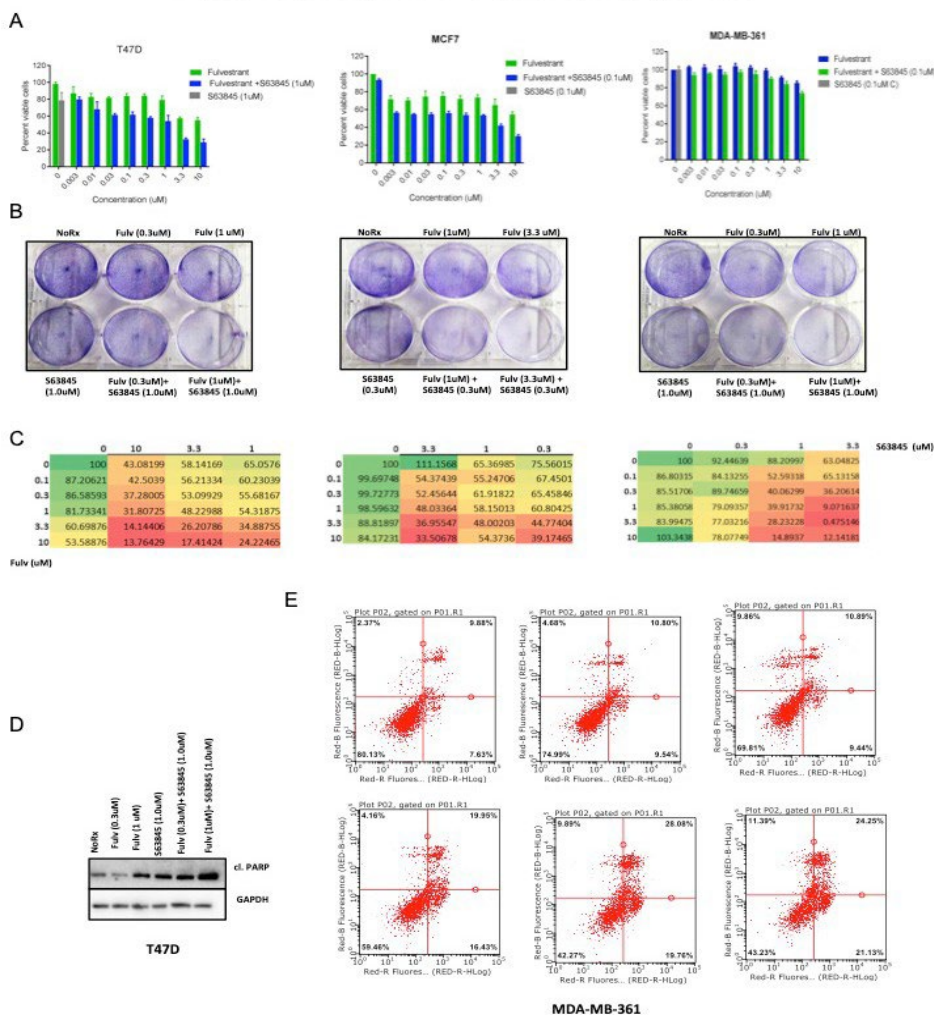


Figure 6. MCL1 inhibition sensitizes ER+ breast cancer to ER inhibition through increased cell death. (A-C) ER+ breast cancer cells T47D, MCF7 and MDA-MB-361 were treated as indicated. C is the Sum-Bliss synergy index scores from (A). (D) Cleaved PARP levels after the indicated treatments. (E) FACS apoptosis of the indicated treatments.

Of note, that, when we overexpressed the other major BCL-2 family proteins, BCL-2 or BCL-xL, we did not see any impact on resistance to HER2 inhibitor, dinaciclib or the combination. (see Floros et al., appended, Sup. Fig. 3). These data demonstrate that dinaciclib works as an MCL-1 inhibitor to sensitize to HER2 inhibitors in HER2 amplified breast cancer, and that MCL-1 is the major anti-apoptotic protein that impacts the ability of HER2 inhibitors to induce cell death and sensitivity.

Lastly, in a mouse model of HER2-amplified BT-474 cells, targeting MCL-1 led to marked sensitization to the tumors to HER2 inhibition (Floros et al., appended, Fig. 4). Overall, MCL-1 is a major resistant factor to HER2 inhibition and its targeting is effective to induce sensitivity to different HER2 inhibitors.

Major Task 2: Characterize the role of the ER-NOXA axis in response to anti-estrogens in ER+ positive breast cancer in vitro and in clinical specimens.

Subtask 1: In the Faber and Scaltriti laboratory, we will determine how the MCL-1 inhibitor S63845 is sensitizing to ER inhibitors

The combination of ER inhibitor with MCL-1 inhibition has been tested: Treatment of the ER+ breast cancer cell lines T47D,

MCF7 and MDA-MB-361 with increasing concentrations of the ER inhibitor fulvestrant in the presence of the MCL1 inhibitor S63845 led to synergistic activity over 72h (Figs. 6A and 6C). In addition, longer crystal violet assays (7d) also evidenced a strong combination effect in these cancers (Fig. 6B). The combination resulted in enhanced apoptotic cell death (Figs. 6D and 6E). These data evidence that MCL1 inhibitors do indeed sensitize ER inhibitors in ER+ breast cancer.

Next, in the ER+ breast cancer cell lines HCC1500 and T47D, we have looked further at BCL-2 member complexes to determine the key changes that underline this sensitivity to ER inhibitors in combination with MCL-1 inhibitors. Indeed, we find consistent with the rest of our data. above in the tumors, fulvestrant increases the amount of MCL-1 bound to BIM (as a result of decreased NOXA levels); S63845 abolishes this complex to induce cell death (Fig. 7).

We next determined the impact of NOXA on the sensitivity of ER inhibition in ER+ breast cancer. Indeed, expression of exogenous NOXA, to prevent its downregulation after ER inhibitor treatment, sensitized (as it leads to downregulation of MCL-1) to ER inhibitor-induced cell death. These data together demonstrate that MCL-1 inhibition leads to sensitization to ER inhibitors through downregulation of ER-NOXA by ER inhibitors (Fig. 8).

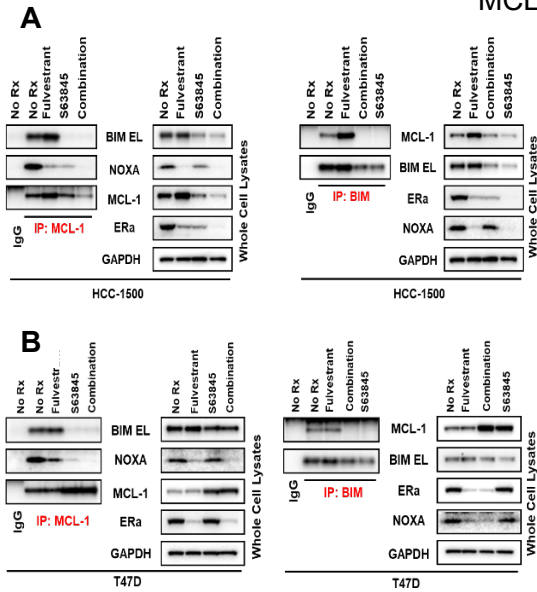


Figure 7. MCL1 inhibitor S63845 disrupts MCL1: BIM complexes. Immunoblots indicate MCL1 and BIM IP performed in (A) HCC-1500 and (B) T47D cells treated with no drug, Fulvestrant, S63845, and their combination.

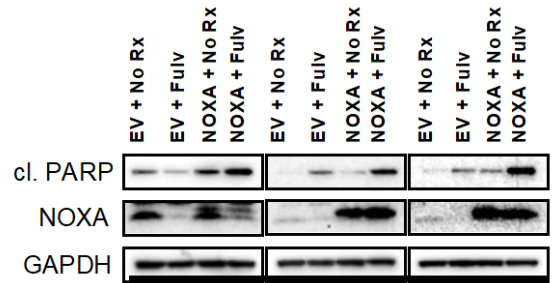


Figure 8. Re-expression of NOXA following ER inhibitor leads to sensitization to cell death. Exogenous NOXA was expressed or control, empty vector (EV) and cells were treated with either nothing (No Rx) or the ER inhibitor fulvestrant (Fulv).

Subtask 2: In collaboration with Drs. Edi Brogi, (Director of Breast Pathology, MSKCC), and Dr. Mikhail Dozmorov (Department of Biostatistics, VCU), we will analyze ~400 ER+ breast cancer samples and 180 HER2+ samples and their relationship to NOXA, MCL-1 and patient outcomes

In the last year of this grant we have expanded on the studies we previously conducted on the study of the NOXA/MCL-1 axis in ER-positive/HER2-negative breast cancer. In previous years, we had reported that ER-positive/HER2-negative breast cancer displaying high NOXA expression had a shorter relapse-free survival (RFS) than patients with NOXA-low breast cancers. Notably, the opposite has observed for MCL-1 (i.e. patients with low – MCL-1 breast cancers had a longer RFS than those with high MCL-1 levels).

To characterize the role of the NOXA/MCL-1 axis in ER-positive/HER2-negative breast cancer further, during the last year of this grant in the Reis-Filho laboratory we conducted i) characterization of the immune infiltration of the cohort of ER-positive/HER2-negative breast cancers previously studied and ii) the analysis of a second cohort of ER-positive/HER2-negative breast cancers with available targeted sequencing data to understand whether the repertoire of genetic alterations of these tumors would vary according to their

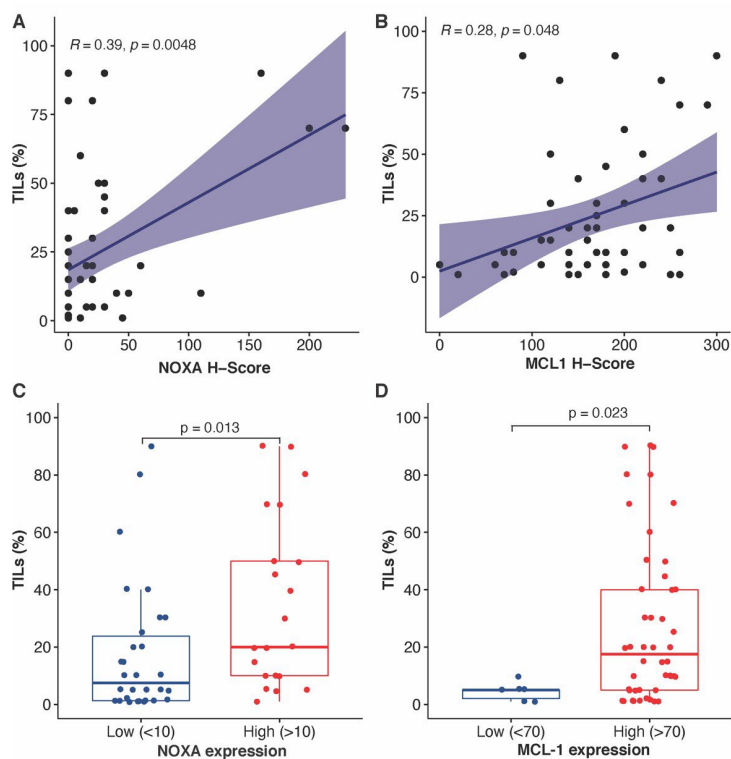


Fig 9. TIL infiltration in ER+/HER2- breast cancer according to NOXA and MCL-1 expression. (A-B) Correlation between (A) NOXA and (B) MCL-1 expression with TIL infiltration. Spearman's test. (C-D) Extent of TIL infiltration in (C) NOXA- high vs NOXA-low and (D) MCL-1 high vs MCL1-low cases according to cut-off determined through maximally selected rank statistic method. Wilcoxon test.

NOXA/MCL-1 expression levels.

We sought to determine whether there would be a relationship between the extent of lymphocytic infiltration (i.e. tumor infiltrating lymphocytes (TILs) and expression of MCL-1 and/or NOXA. We evaluated TILs in the breast cancer samples in our cohort following the recommendations and guidelines for histopathologic assessment of TILs provided by the International TILs Working Group (PMID: 25214542). Following the definition of stromal TILs, the % reported represent the fraction of intratumoral stromal area covered by mononuclear immune cells. TIL evaluation was conducted in one representative tissue section per case by a board-certified Pathologist.

Our analyses revealed a significant positive correlation between the extent of TIL infiltration and both NOXA ($R=0.39$, $P=0.005$; and MCL1 expression ($R=0.28$, $P=0.048$; **Fig. 9A-9B**). Subsequently, we stratified the breast cancer samples as NOXA-high and NOXA-low, and as MCL1-high and MCL1-low using the H-score cutoffs (NOXA, H-score=10; MCL1, H-score=70) which we derived, as detailed in the previous reports, using the maximally selected rank statistics and that were found to be associated with the most significant differences in RFS. We observed that ER-positive/HER2-negative breast cancer samples displaying a 'high NOXA expression' (H-score >10) showed a higher extent of TIL infiltration compared to

those tumors with a 'low NOXA expression' (H-score <10; mean TILs 33.9% vs 17.7%; $P=0.01$). Similarly, the extent of TIL infiltration in MCL-1-high ER- positive/HER2-negative breast cancers was significantly higher than that in MCL-1-low tumors (mean TILs 27.1% vs 4.5%, $P=0.02$; **Fig. 9C-9D and Fig 10A-F**). Crosstalks between NOXA-MCL-1 axis and the immune system have been reported (PMID: 29053140, 20620942, 27762293). It is possible that signaling through this axis in tumor cells has an effect in the tumor

microenvironment (TME). Alternatively, the TME might affect the activation of the NOXA-MCL-1 axis in the tumor cells. Future work to determine the composition of the TME according to NOXA/MCL-1 expression, and studies on the role of this axis in regulating the immune response of breast cancers is warranted.

We next investigated the repertoire of genetic alterations in ER-positive/HER2-negative breast cancers would vary according to the expression of NOXA/MCL-1 in breast cancer. We conducted the evaluation of NOXA and MCL-1 expression by immunohistochemistry in a cohort of 61 ER-positive/HER2-negative breast cancers that had been previously subjected to targeted sequencing using the Memorial Sloan Kettering

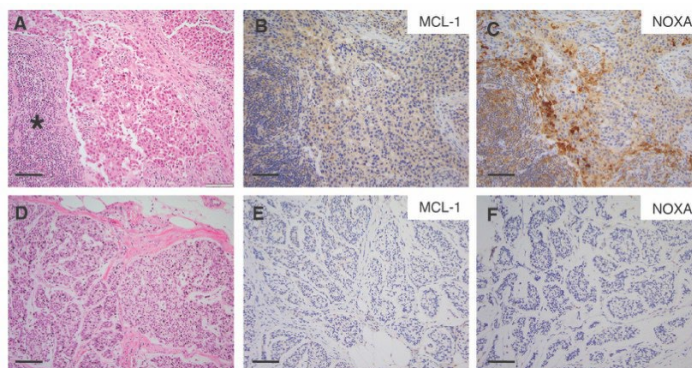


Fig 10. Representative H&E micrographs of ER-positive/HER2-negative cases showing (A, D) and MCL-1 (B, E) and NOXA (C, F) expression depicting the higher TIL infiltration in an MCL1-high and NOXA-high case. *, tumor infiltrating lymphocytes. Scale bar, 50 microns

Integrated Mutation Profiling of Actionable Cancer Targets (MSK-IMPACT) assay. IHC was conducted following the protocols previously established in this work). Targeted sequencing data were analyzed in the Reis-Filho laboratory using a validated bioinformatic pipeline (PMID: 29506079, 33083532, 30166553).

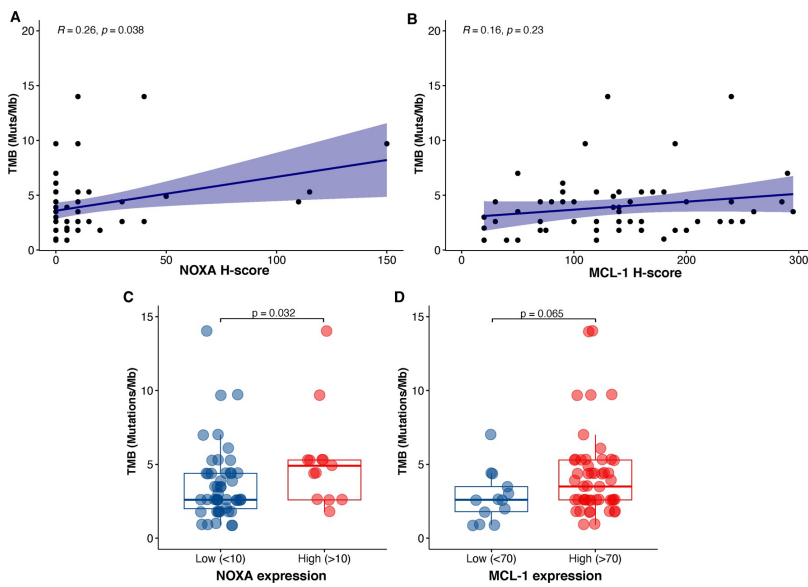


Fig 11. Tumor mutation burden (TMB) according to NOXA/MCL-1 expression. (A-B) Correlation between TMB and NOXA (A) and MCL-1 (B) expression by IHC. Spearman's test. (C-D) TMB in (C) NOXA-high vs NOXA-low and (D) MCL-1 high vs MCL1-low cases according to cut-off determined through maximally selected rank statistic method. Wilcoxon test.

Our analysis revealed a positive correlation between NOXA expression and tumor mutational burden (TMB; $R = 0.26$, $P = 0.038$). In agreement with these findings, those cases displaying a high expression of NOXA (H-score >10), according to the cutoff based on the maximally selected rank statistics derived from our analyses in previous cohort of ER-positive/HER2-negative breast cancers we studied had a statistically significantly higher TMB than NOXA-low breast cancers (H-score <10; median 4.9 vs 2.6 mutations/Mb; $P=0.032$; Mann Whitney U-test; **Fig 9A, 9C**). Although MCL-1-high cases showed a numerically higher TMB than MCL1-low cases, this was not statistically significant (median TMB 3.5 vs 2.6 mut/Mb, $p=0.06$) and no significant correlation was seen between TMB and MCL-1 expression ($R = 0.16$, $p = 0.23$; **Fig 11B, 11D**).

The genes most frequently affected by pathogenic genetic alterations in NOXA-high cases were *WHSC1L1*, *GATA3* and *CCND1* (5/13; 39% each) and those most frequently altered in NOXA-low cases were *PIK3CA* (18/48; 38%), *TP53* (16/48; 33.3%), and *FGF19* and *CDH1* (10/48; 21%, each; **Fig 12**). We observed notable differences between NOXA- high and NOXA-low cases, such a statistically significant enrichment in NOXA-high samples in pathogenic genetic alterations affecting the chromatin remodeler *WHSC1L1* (38.5% vs 8.3%, $P=0.02$), *BAP1* (15.4% vs 0%, $P=0.04$) that

besides its role in DNA repair plays key roles in chromatin remodeling, and in *PRKAR1A* (15.4% vs 0%, $P=0.04$), which encodes for the cAMP- dependent protein kinase type I-alpha regulatory subunit (**Fig. 13A**). *TP53* (17/49; 35%), *PIK3CA* (16/49; 33%), and *FGF19*, *FGF3* and *FGF4*

(11/49; 22%) were the most frequently altered genes in MCL-1-high cases, whereas *PIK3CA* and *CDH1* were the genes most frequently affected in MCL-1-low cases (**Fig. 12**). No statistically significant differences were identified according to MCL-1 expression (**Fig. 13B**). These data indicate that the NOXA/MCL-1 axis might crosstalk with biological processes involved in the modification of chromatin architecture. Further studies validating this notion and exploring the role of this axis in transcriptional control through chromatin remodeling are warranted.

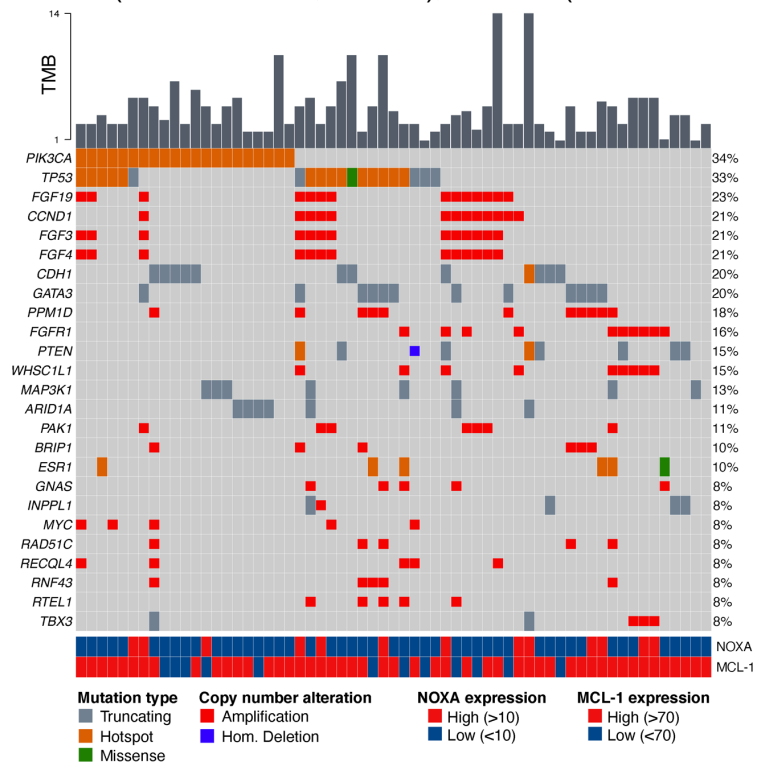


Fig 12. Repertoire of somatic genetic alteration in ER+/HER2- breast cancers according to NOXA and MCL-1 expression. Oncoprint depicting the genes most frequently affected by pathogenic genetic alterations in the cohort. NOXA and MCL-1 expression by IHC is shown in a phenobar (bottom).

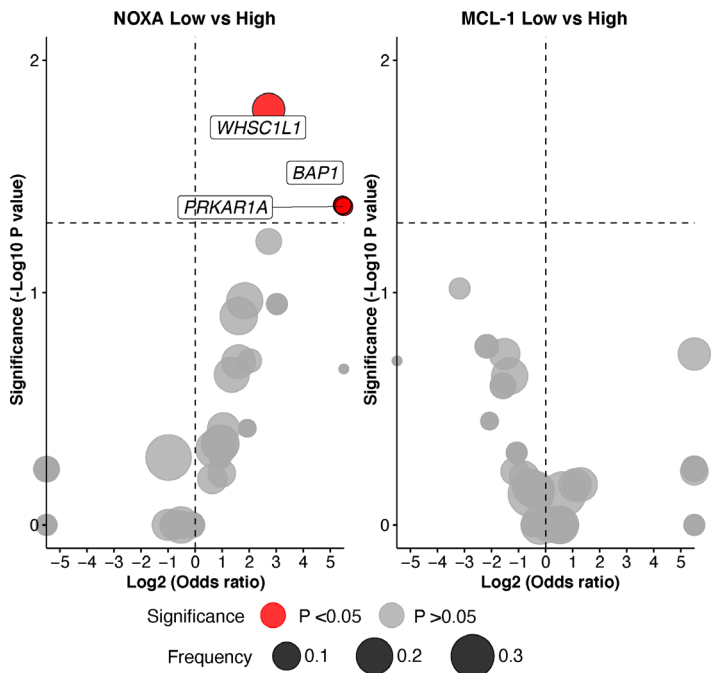


Fig 13. Enrichment of pathogenic genetic alterations in NOXA- high vs NOXA-low ER+/HER2- breast cancers (left) and in MCL1-high vs MCL1-low tumors (right)

The higher frequency of *CDH1* and *PIK3CA* mutations in MCL-1-low cancers suggested that this group is enriched for invasive lobular carcinomas, which harbor *CDH1* mutations in up to 80% of cases and are also relatively enriched for *PIK3CA* mutations. To test this hypothesis, we compared the distribution of invasive lobular carcinomas and invasive ductal carcinomas of no special type, according to the expression of NOXA and MCL-1. Consistent with the associations revealed by genomic analysis, although not statistically significant, a numerically higher proportion of MCL-1 low breast cancers (31% in MCL-1 low vs 11% of MCL-1 high) cancers displayed an invasive lobular carcinoma histologic type.

Subtask 3: In the Faber and Scaltriti laboratory, we will determine if microRNA 4728 is responsible for NOXA downregulation via estrogen receptor downregulation. These experiments will include miRNA quantification, miRNA silencing experiments, and miRNA overexpression experiments

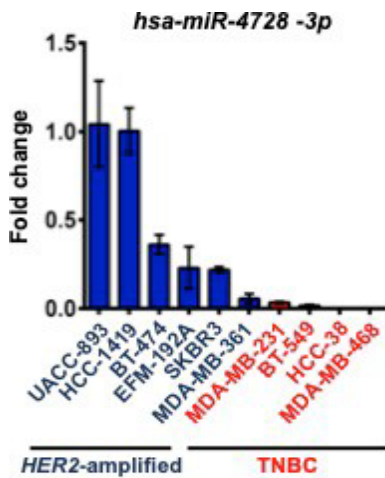


Fig. 14. miRNA4728 is overexpressed in HER2-amplified breast cancer. qPCR was performed to quantify miRNA4728, relative to an miRNA housekeeping gene.

We first quantified miRNA4728, We found markedly higher levels in HER2-amplified breast cancer cell lines, compared to triple negative breast cancer, consistent with our demonstration that it is amplified intragenic on the *HER2* amplicon (Fig. 14).

To study the function of miRNA4728, we conducted a series of manipulation experiments (inhibition and overexpression). Briefly we transduced virus with a miRNA4728 locker inhibitor) and control, or, a miRNA4728 expression vector (or control). In HER2+/ER+ BT474 and MDA-MB-361 breast cancer cell lines, the HER2+/ER- SKBR3 cells, and the HER2-/ER+ T47D cells. In all cases, miRNA4728 inhibitor increased both ER and NOXA when compared to control; in all cases, overexpression of miRNA4728 leads to downregulation of ER and NOXA, when compared to control (Fig. 15A and 15B). Treatment with the ER inhibitor fulvestrant led to downregulation of ER and NOXA, as previously demonstrated in this report, however, the miRNA4728 inhibitor mitigated the downregulation of NOXA (Fig. 15C). Similarly, miRNA4728 inhibitor prevented NOXA

downregulation following treatment with the HER2 inhibitor, lapatinib (Fig. 14D). Impressively, as a result, these cells were sensitized to lapatinib as evidenced by cleaved PARP (Fig. 15D and 15E).

Conversely, overexpression of miRNA4728 sensitized to lapatinib (Fig. 15E). These data demonstrate that miRNA4728 controls NOXA expression, and when manipulated, impacts NOXA expression and sensitivity to HER2 inhibitors.

Major Task 3: Assess the efficacy of dual HER2 and MCL-1 inhibition in diverse *HER2* amplified breast PDX models and dual ER and MCL-1 inhibition in diverse ER+ breast PDX models.

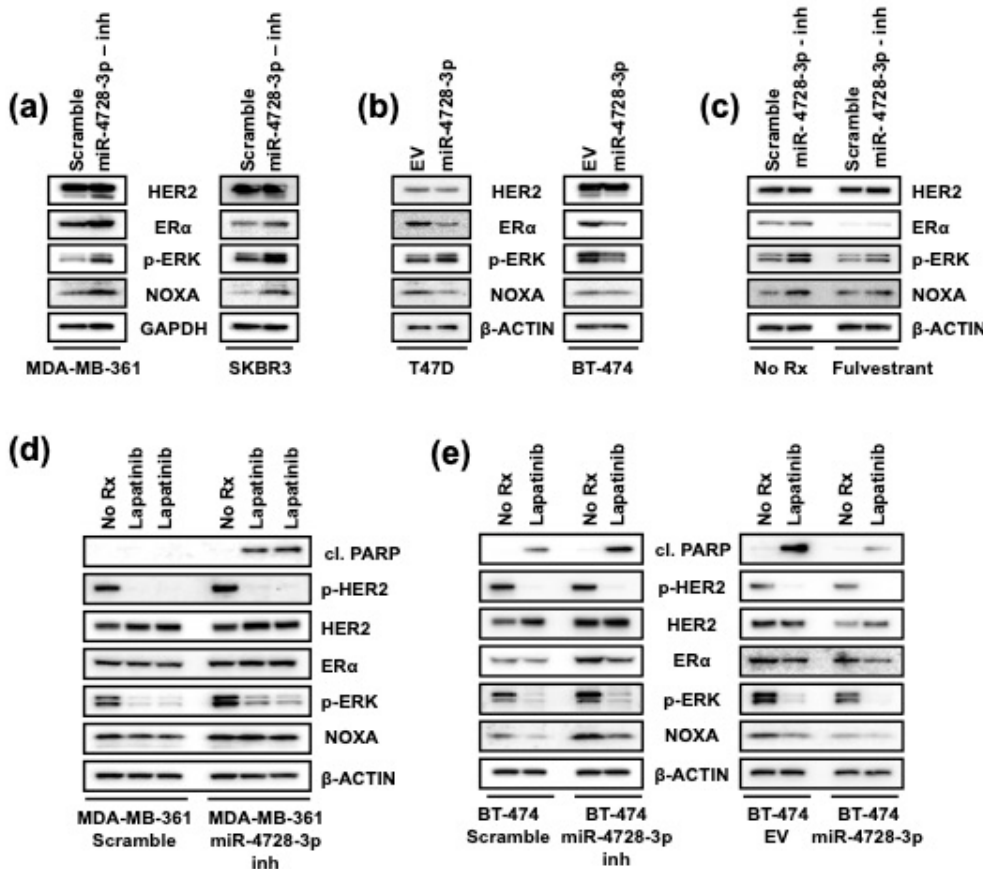
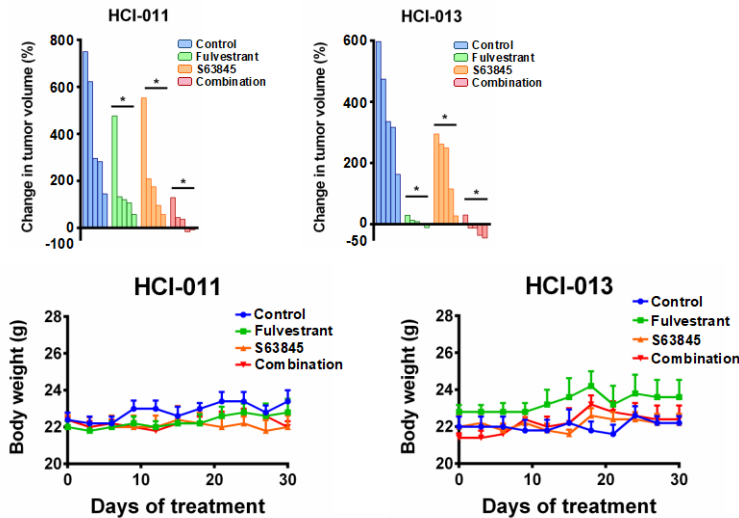


Figure 15. Manipulation of miRNA4728 effects NOXA expression in breast cancer. (A) knockdown of miRNA4728 leads to upregulation of the expression of the ER and NOXA. (B) Exogenous expression of miRNA4728 leads to lower ER and NOXA expression. (C) Knockdown of miRNA4728 leads to upregulation of the expression of the ER and NOXA but not in the presence of the ER inhibitor fulvestrant. (D and E) knockdown of miRNA4728 leads to upregulation of the expression of the ER and NOXA and subsequent sensitization to the HER2 inhibition lapatinib in HER2 amplified breast cancer cells, while further overexpression mitigates sensitivity (Sensitivity/cell death is determined by CI PARP levels).

Subtask 1: In the Faber and Scaltriti laboratory, we will characterize the *in vivo* activity of HER2i/MCL-1i in HER2 amplified breast PDX models.

We tested neratinib in combination with dinaciclib in two *HER2*-amplified PDX models (WHIM 8 and WHIM 22). While neratinib was effective at blocking the growth of the *HER2*-amplified tumors, the combination of dinaciclib and neratinib was superior to single-agent therapy in the WHIM 22 model (Floros et al., appended, Fig. 5A). In addition, there was no weight loss of the mice treated with the single agents or the combination (Floros et al., appended, Fig. 5B), again suggesting tolerability. In the WHIM 8 model, we observed high activity of neratinib monotherapy; however, the combination of neratinib and dinaciclib resulted in uniformly robust tumor shrinkage (>50%), with mice again not showing any significant weight loss (Floros et al., appended, Fig. 5C-5D). Cleaved PARP was elevated when the two drugs were administered together, indicating induction of apoptosis, while reduction of p-HER2 and MCL-1 advocates for the on-target effect of neratinib and dinaciclib, respectively (Floros et al., appended, Fig. 5E). These data demonstrate potent combination efficacy of neratinib and dinaciclib in *HER2*-positive breast cancer PDX models.



Subtask 2: In the Faber and Koblinski laboratory, we will characterize the *in vivo* activity of HER2 antibodies/MCL-1i humanized mouse model studies

As mentioned above, several ADCs have essentially replaced Abs as standard-of-care. Thus, we found these experiments were not relevant.

Figure 16. Estrogen inhibitor plus S63845 is effective in ER+ PDX models.

Approximately 2×10^6 cells derived from two PDX ER+ breast cancer models (H) HCl-011 and (I) HCl-013 were injected into the fourth mammary fat pads of experimental female NSG mice and monitored for subsequent growth. After tumors reached a size of $\sim 150 \text{ mm}^3$, mice were treated with 5mg/body/week of fulvestrant or/and with 25mg/kg of S63845 biweekly for 3 weeks. Tumors were measured daily by caliper, in two dimensions (length and width), and tumor volume was calculated with the formula $v = l \times (w)^2 (\pi/6)$, where v is the tumor volume, l is the length, and w is the width (the smaller of the two measurements). Waterfall plots indicate percentage change in tumor volume (control, 5 tumors; fulvestrant, 5 tumors; S63845, 5 tumors; combination, 5 tumors) of HCl-011 and HCl-013 ER+ PDX models respectively. For statistical analysis one-way Anova test was performed for comparisons between fulvestrant, S63845 and combination cohorts. Dunnett's test was used as post hoc. Differences were considered statistically different if $p < 0.05$. A p -value < 0.05 is indicated by *, $p < 0.01$ by **, $p <$

Subtask 3: In the Faber and Scaltriti laboratory, we will characterize the *in vivo* activity of ER inhibitors/MCL-1i in ER+ breast cancers

We next investigated the efficacy of our combination therapeutic strategy in two patient-derived xenograft (PDX) models of metastatic ER+ breast cancer, termed HCl-011 and HCl-013. Tumor-bearing mice with estrogen pellets were randomized and divided into four group: treatments with vehicle, fulvestrant, S63845, or the combination. Fulvestrant was administered subcutaneously at a concentration of 5 mg/body/wk, and S63845 was administered intravenously biweekly at a concentration of 25mg/kg⁵. While fulvestrant was effective at blocking the growth of ER+ breast tumors, as would be expected, the combination of fulvestrant and S63845 was superior to single agent therapy in both the ER+ PDX models (Fig. 17). Additionally, the combination was well tolerated (Fig. 17). Single agent MCL-1 inhibitor was not effective in both PDX models but when treated in combination with fulvestrant, HCl-011 PDX showed significant tumor shrinkage (>50%). These data therefore demonstrate potent combination efficacy of fulvestrant and S63845 in ER+ positive breast cancer PDX models.

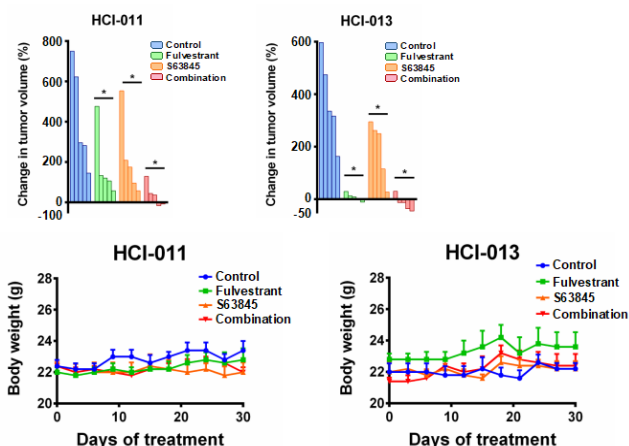


Figure 17. ER+ breast cancer PDX models are sensitive to ER inhibitor + MCL-1 inhibitor. (Top) Waterfall plots of two ER+ PDX models. Each line represents a unique tumor and their response during 30d of treatment. (Bottom) The weights of the mice during treatment.

free survival supports the testing of pharmacologic intervention targeting the NOXA/MCL-1 axis in these tumors. Furthermore, the novel observations related to the differences in the repertoire of genetic alterations as well as histologic types in ER+/HER2- breast cancers according to NOXA/MCL-1 expression, in particular our finding of an enrichment of pathogenic alterations in chromatin remodelers in NOXA-high samples open new avenues for the investigation on the interactions between the NOXA/MCL-1 axis and chromatin modification.

5. Changes/Problems

Given the success of novel anti-HER2 ADCs in *HER2* amplified breast cancer, during the last year of this grant we focused on the study of NOXA/MCL-1 in ER-positive/HER2-negative breast cancers and not on HER2 antibody studies in vivo.

6. Products

-Targeting transcription of MCL-1

sensitizes HER2-amplified breast cancers to HER2 inhibitors Floros KV, Jacob S, Kurupi R, Fairchild CK, Hu B, Puchalapalli M, Koblinski J, Dozmorov MG, Boikos SA, Scaltriti M, Faber AC. *Cell Death Dis.* 2021 Feb 15; 12(2):179. PMID: [33589591](https://pubmed.ncbi.nlm.nih.gov/33589591/).

-Adaptive resistance to ER inhibition is overcome by targeting MCL-1

Konstantinos V. Floros^a, Sheeba Jacob^a, Bin Hu^b, Madhavi Puchalapalli^b, Mohammad A. Alzub^{b,c}, Sosipatros A. Boikos^d, Edi Brogi^e, Sarat Chandrapaty^e, Jennifer E. Koblinski^b, J. Chuck Harrell^{b,c,f}, Maurizio Scaltriti^{e,g,h}, and Anthony C. Faber^a *Manuscript submitted*

- ER-positive/HER2-negative breast cancer and the NOXA/MCL1 axis: A genomic characterization.

Antonio Marra, Higinio Dopeso, Fresia Pareja, Achim Jungbluth, Edi Brogi, Maurizio Scaltriti, Anthony Faber, Jorge S. Reis-Filho. *Manuscript in preparation*

7. Participants & Other Collaborating Organizations

The SOW has been faithfully followed for the contributions of VCU and MSKCC The following individuals have worked on the grant at VCU:

- 1) Name: Anthony Faber Project Role: Lead PI
Nearest person month worked: 2

Dr. Faber oversees the everyday experimentation in the laboratory related to the proposal

4. Impact

Taken together, the data we have generated throughout this grant demonstrate that the addition of an MCL-1 inhibitor (both S63845 or dinaciclib), which a number are in clinical testing, sensitizes ER-positive breast cancer to ER inhibitors. In addition, we have characterized a miRNA4728-NOXA-MCL-1 axis that controls NOXA expression and MCL-1 addiction in *HER2* amplified breast cancer models and ER+ breast cancer models. Importantly, both HER2 inhibition and ER inhibition leads to NOXA downregulation and a MCL-1 dependence. These data are particularly interesting in light of the VERONICA trial, in which a BCL-2 inhibitor accelerated ER+ breast cancer disease. **This is consistent with our data that these cancers are dependent on MCL-1, and not BCL-2.** All in all, this sets the stage for clinical evaluation of HER2 inhibitors and MCL-1 inhibitors and ER inhibitors and MCL-1 inhibitors in breast cancer.

Moreover, our findings that NOXA-high and MCL1-low ER+/HER2- breast cancers have a shorter recurrence-

- 2) Name: Sheeba Jacobs
Project role: Postdoctoral Fellow Nearest person month worked: 9
Dr. Jacobs participates in all aims at VCU as a scientist in the laboratory
- 3) Jennifer Ramachandran (Koblinski) Project role: co-I
Nearest person month worked: 1
Dr. Ramachandran assists in all mouse-related work and pathology at VCU
- 4) Mikhail Dozmorov Project role: co-I
Nearest person month worked: 1
Dr. Dozmorov assists in all statistical matters for this grant

The following individuals have worked on the grant at MSK:

1) Jorge Reis-Filho

Project Role: Partnering PI Nearest person month worked: 2

Dr. Reis-Filho oversees all day-to-day experimentation in the laboratory related to this proposal and oversees the design and data analysis.

Funding Support: This award (W81XWH-18-1-0562)

Sarat Chandarlapaty

Project Role: Co-Investigator Nearest person month worked: 1

Dr. Chandarlapaty directs the efforts in his laboratory on developing model systems, collects human samples from breast cancer patients treated at MSKCC and assesses the benefit of different therapeutic strategies.

Funding Support: This award (W81XWH-18-1-0562)

Edi Brogi

Project Role: Co-Investigator Nearest person month worked: 1

Dr. Brogi analyzes tissue samples from breast cancer patients undergoing treatment and evaluates the purity of cancer tissues and performs immunohistochemistry assays.

Funding Support: This award (W81XWH-18-1-0562)

Yanyan Cai

Project Role: Research Scholar Nearest person month worked: 4

Dr. Cai, a postdoctoral scholar, leads all lab experiments, coordinates with genomics core and was responsible for animal work.

Funding Support: This award (W81XWH-18-1-0562)

Shirin Issa Bhaloo

Project Role: Research Associate Nearest person month worked: 3

Dr. Issa Bhaloo is a Research Associate in the Reis-Filho Lab who assists with all aspects of this proposal, including tissue culture, cloning, biochemical assays, maintenance of patient-derived models needed for in vivo studies and sample preparation for sequencing.

Funding Support: This award (W81XWH-18-1-0562)

8. Special Reporting and Requirements: N/A

Transition Plan Questionnaire

Directions: Please answer all questions that apply for each product under development. Please fill out one document per product. *This is not an application for funding; however, answers will help us understand the outcomes and products from your award.*

1. After the award closes, would you be willing to periodically provide voluntary information (via email) regarding the project status (i.e. where the research is headed)? **Yes** or **No**

These responses will help CDMRP demonstrate the return on its investments and will help demonstrate that the CDMRP is a responsible and successful steward of federal research funding.

2. What **conclusion(s)** does your final data support?

3. Will you/have you applied for/obtained follow-on-funding for this project? **If yes**, please list (a) funding organization, (b) total budget requested/obtained, and (c) title of the funded proposal. *This information will be recorded as an outcome to this award.*

4. What will be **the next step(s)** for this project?

5. How would you classify your **lead candidate product**? *Please choose the best option or add explanation for multiple selections.*

(a) Therapeutic (Small Molecule, Biologic, Cell/Gene Therapy):

(b) Diagnostic

(c) Device

(d) Research Tool to Address a Research Bottleneck

(e) Knowledge Product (Non-material product such as a compound library, database, something that improves clinical practice, education, etc.)

(f) Other - Please Specify:

6. How does your candidate product aid the Warfighter, Veteran, Beneficiary, and/or General Population?

7. Therapy / Product Development, Transition Strategies, and Intellectual Property

Describe the steps and relevant strategies required to move the candidate product (knowledge or tangible) to the next phase of development and/or commercialization. Please address any issues with intellectual property.

PIs are encouraged to explore the technical requirements and the current regulatory strategies involved in product development as well as to work with their organization's Technology Transfer Office (or equivalent regulatory/legal office), federal/international regulatory experts, to develop the transition plan and to explore developing relationships with industry, DoD advanced developers (e.g. USAMMDA), and/or other funding agencies to facilitate moving the product into the next phase.

ARTICLE

Open Access

Targeting transcription of *MCL-1* sensitizes *HER2*-amplified breast cancers to *HER2* inhibitors

Konstantinos V. Floros¹, Sheeba Jacob¹, Richard Kurupi¹, Carter K. Fairchild¹, Bin Hu², Madhavi Puchalapalli², Jennifer E. Koblinski², Mikhail G. Dozmorov³, Sosipatros A. Boikos⁴, Maurizio Scaltriti^{5,6,7} and Anthony C. Faber¹

Abstract

Human epidermal growth factor receptor 2 gene (*HER2*) is focally amplified in approximately 20% of breast cancers. *HER2* inhibitors alone are not effective, and sensitizing agents will be necessary to move away from a reliance on heavily toxic chemotherapeutics. We recently demonstrated that the efficacy of *HER2* inhibitors is mitigated by uniformly low levels of the myeloid cell leukemia 1 (*MCL-1*) endogenous inhibitor, NOXA. Emerging clinical data have demonstrated that clinically advanced cyclin-dependent kinase (CDK) inhibitors are effective *MCL-1* inhibitors in patients, and, importantly, well tolerated. We, therefore, tested whether the CDK inhibitor, dinaciclib, could block *MCL-1* in preclinical *HER2*-amplified breast cancer models and therefore sensitize these cancers to dual *HER2/EGFR* inhibitors neratinib and lapatinib, as well as to the novel selective *HER2* inhibitor tucatinib. Indeed, we found dinaciclib suppresses *MCL-1* RNA and is highly effective at sensitizing *HER2* inhibitors both in vitro and in vivo. This combination was tolerable in vivo. Mechanistically, liberating the effector BCL-2 protein, BAK, from *MCL-1* results in robust apoptosis. Thus, clinically advanced CDK inhibitors may effectively combine with *HER2* inhibitors and present a chemotherapy-free therapeutic strategy in *HER2*-amplified breast cancer, which can be tested immediately in the clinic.

Introduction

HER2 inhibitors extend survival in *HER2*-amplified breast cancers; however, they are not sufficiently active as monotherapy^{1,2}, unlike other receptor tyrosine kinase (RTK) inhibitors in solid tumor cancer paradigms. Due to this, there remains a reliance on chemotherapy; in contrast, in paradigms like epidermal growth factor receptor (*EGFR*)-mutant lung cancer and anaplastic lymphoma kinase (*ALK*)-translocated lung cancer, effective targeted therapy has mitigated the need of chemotherapy³.

We have demonstrated recently that *HER2*-amplified breast cancers have significantly lower NOXA levels, leading to *MCL-1*-mediated resistance to *HER2* inhibitors through suppression of apoptosis⁴. Similarly, Merino et al.⁵ demonstrated that co-administration of *MCL-1* inhibitors with *HER2* inhibitors sensitizes *HER2*-amplified breast cancer models. While *MCL-1* BH3 mimetics are advancing into clinical trials either alone or with venetoclax in hematological cancers, it remains uncertain whether these drugs will be able to sufficiently block the interaction of *MCL-1* and proapoptotic BH3-only proteins such as NOXA and BIM. Moreover, the tolerability of these drugs in combination is unknown.

Inhibitors that block CDK9 can interfere with gene transcription. Thus, transcription of mRNAs with short half-lives that need to be synthesized at a high rate may be particularly affected by these agents⁶. Unique among the antiapoptotic proteins, *MCL-1* has a very short half-life^{7,8}. Dinaciclib has been used as an *MCL-1* inhibitor in several cancer paradigms. It has already been reported that

Correspondence: Anthony C. Faber (acfaber@vcu.edu)

¹Department of Oral and Craniofacial Molecular Biology, Phillips Institute for Oral Health Research, VCU School of Dentistry and Massey Cancer Center, Virginia Commonwealth University, Richmond, VA 23298, USA

²Department of Pathology, Virginia Commonwealth University School of Medicine and Massey Cancer Center, Richmond, VA 23220, USA

Full list of author information is available at the end of the article

These authors contributed equally: Konstantinos V. Floros, Sheeba Jacob, Richard Kurupi

Edited by L. Galluzzi

© The Author(s) 2021



Open Access This article is licensed under a Creative Commons Attribution 4.0 International License, which permits use, sharing, adaptation, distribution and reproduction in any medium or format, as long as you give appropriate credit to the original author(s) and the source, provide a link to the Creative Commons license, and indicate if changes were made. The images or other third party material in this article are included in the article's Creative Commons license, unless indicated otherwise in a credit line to the material. If material is not included in the article's Creative Commons license and your intended use is not permitted by statutory regulation or exceeds the permitted use, you will need to obtain permission directly from the copyright holder. To view a copy of this license, visit <http://creativecommons.org/licenses/by/4.0/>.

dinaciclib causes mitochondria-dependent apoptosis in osteosarcoma with MCL-1 being the primary target⁹, and in hepatocellular carcinoma dinaciclib decreases *MCL-1* mRNA levels without significantly changing the expression of other BCL-2 proteins¹⁰. Interestingly, CDK9 inhibition with dinaciclib is highly effective in MYC-driven lymphomas and involves downregulation of MCL-1¹¹. And while there are also studies that support the elimination of MCL-1 at the protein level as the potential mechanism of action of dinaciclib¹², most advocate for transcriptional downregulation of *MCL-1* as the critical mechanism^{9,13}. In addition, we have recently demonstrated that the CDK inhibitor dinaciclib effectively blocks MCL-1 to sensitize EGFR inhibitors in *EGFR*-mutant non-small cell lung cancer (NSCLC)¹⁴. Dinaciclib exposure time peaks are roughly 2 h in humans, which is sufficient to block MCL-1, but not sufficient to block CDK1 or CDK2¹⁵. This suggests that the anticancer activity seen with dinaciclib is a result of its inhibitory effect on CDK9, and not CDK1/2. In a phase I trial in breast cancer patients, neutropenia and leukopenia were common, but dinaciclib in general was well tolerated¹⁶. In this study, we aimed to explore whether dinaciclib was sufficient to sensitize preclinical models of *HER2*-amplified breast cancer through downregulation of MCL-1.

Results

Dinaciclib sensitizes *HER2*-amplified breast cancers to *HER2* inhibitors and is superior to the MCL-1 BH3 mimetic A-1210477

We and others recently demonstrated that pharmacological inhibitors of MCL-1 sensitized *HER2* inhibitors in *HER2*-amplified breast cancers^{4,5}. Based both on dinaciclib's ability to inhibit MCL-1 in vitro and in vivo and its intrinsic therapeutic window, we investigated whether dinaciclib could be added to *HER2* inhibitors and sensitize them through downregulation of MCL-1. In both *HER2*-amplified BT-474 and MDA-MB-453 cells, dinaciclib effectively reduced MCL-1 expression (Fig. 1A). In both cell lines, dinaciclib was more potent as a combining partner with the *HER2* inhibitor lapatinib than was the MCL-1 BH3 mimetic A-1210477, as evidenced by cleaved PARP levels, a marker for apoptosis (Fig. 1A). In addition, while phosphorylation of *HER2* was completely abolished, consistent with the on-target effect of lapatinib, *HER2* levels were not significantly altered with any of the drug treatments (Fig. 1A). As expected, both the *HER2*/PI3K/TORC1 and *HER2*/RAS/TORC1 signaling pathways were disrupted by *HER2* kinase inhibition, as evidenced by loss of pHER2, p-AKT (PI3K readout), p-ERK (RAS pathway readout), and p-S6 loss (mTORC1 pathway readout)¹⁷ (Fig. 1A). Dinaciclib strongly activated PI3K and MEK signaling, as evidenced by increased p-AKT (308) and p-ERK, respectively. However, lapatinib eventually

abrogated both feedback activations (Fig. 1A). Of note, downregulation of MCL-1 by dinaciclib destabilizes also BIM EL (Fig. 1A), which was also noticed in our previous studies⁴.

In order to corroborate previous reports that dinaciclib-induced MCL-1 decreases are due to loss of MCL-1 transcription¹⁰, we evaluated *MCL-1* mRNA expression after treating different *HER2*-amplified breast cancer cell lines with dinaciclib (Fig. 1B). As expected, *MCL-1* mRNA expression was suppressed 2 h after dinaciclib addition. Consistently, after treating BT-474 cells for 24 h and the less sensitive MDA-MB-453 cells for 72 h, cell viability decreased more with the combination of lapatinib and dinaciclib than with lapatinib and A-1210477 (Fig. 1C). We further determined the sensitivity of the *HER2*-amplified breast cancer cell lines to the different combinations of these agents to gain information regarding the contribution of each single agent to the observed toxicity (Supplementary Fig. 1). In line with our previous data, dinaciclib displays a more synergistic potential with lapatinib than A-1210477 does. Altogether, these data indicate that dinaciclib downregulates MCL-1 and sensitizes to *HER2* inhibitor in *HER2*-amplified breast cancers. Given that PARP cleavage has been reported to be implicated in other non-apoptotic processes^{18,19} and MCL-1 also exhibits apoptosis-independent functions in the cell^{20,21}, we assessed Annexin V positivity by flow cytometry to confirm toxicity from loss of MCL-1 was due to an increase in apoptosis (Fig. 1D and Supplementary Fig. 2). To gain mechanistic insight, we immunoprecipitated MCL-1 in the BT-474 and MDA-MB-453 cells and observed that dinaciclib toxicity is mediated at least in part by BAK, which is liberated from MCL-1 following treatment and is free to execute its apoptotic program (Fig. 1E). Potential alterations in BIM EL:MCL-1 complexes were also investigated since BIM EL is a direct activator of Bcl-2-associated X protein (BAX)/Bcl-2 homologous antagonist/killer (BAK) molecules and its liberation could lead to further cell death responses. However, consistent with our previous data²², BIM EL levels were significantly downregulated in the whole-cell lysates following the addition of dinaciclib (Fig. 1E) making likely its role in combination toxicity, if any, limited.

Dinaciclib sensitization to *HER2*-amplified breast cancers is abrogated by BAK knockdown and largely mediated by MCL-1

As BAK-MCL-1 was sharply disrupted by dinaciclib, we sought to investigate this complex further and the role, if any, of BAK in dinaciclib and *HER2* inhibitor/dinaciclib toxicity. Mechanistically, MCL-1 binds to BAK to prevent its activation²³. Thus, if MCL-1 is critical to combination activity, BAK knockdown should mitigate the activity of

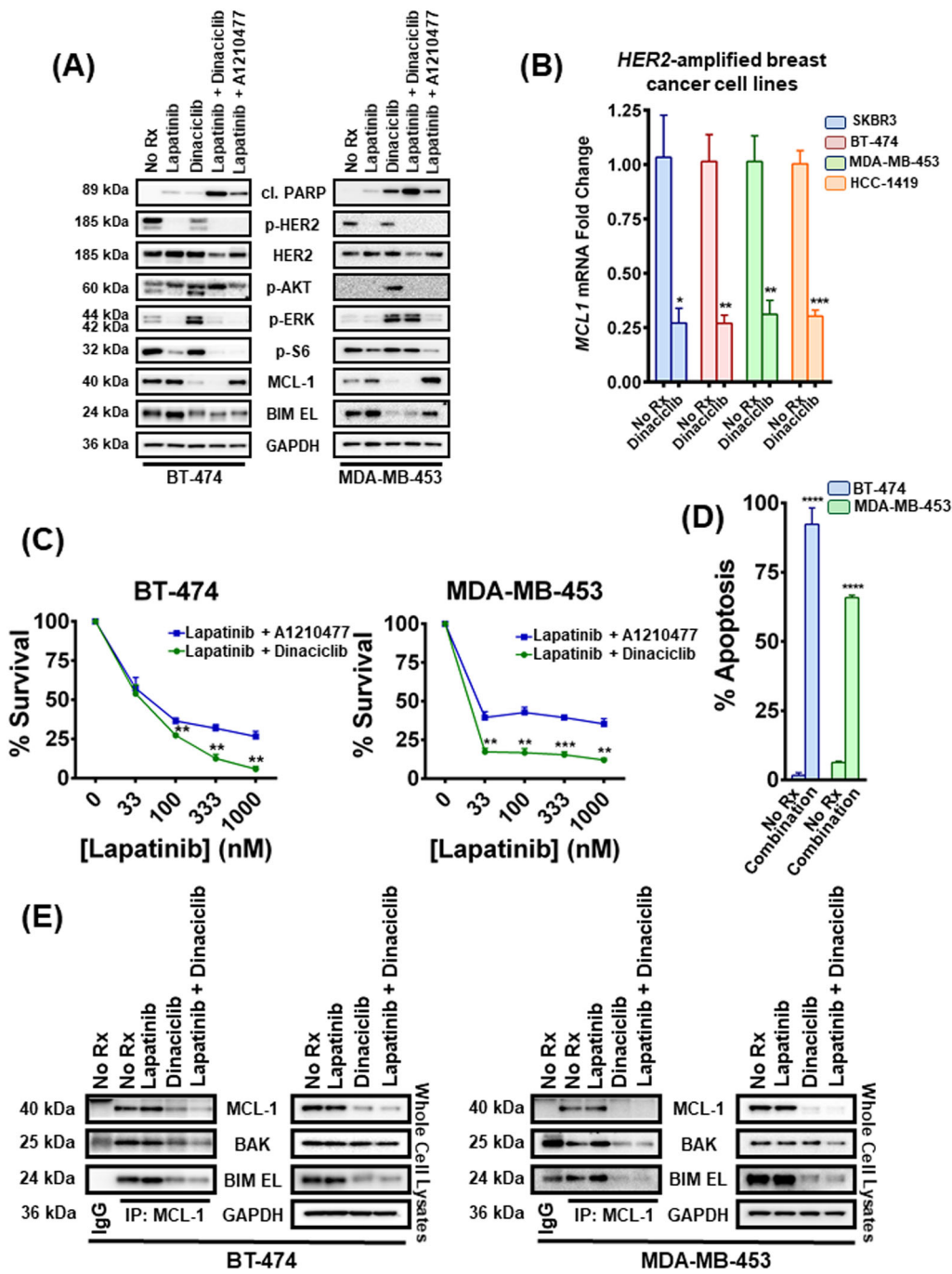


Fig. 1 Dinaciclib sensitizes *HER2*-amplified breast cancer cells to lapatinib and liberates BAK from MCL-1. **A** BT-474 and MDA-MB-453 cells were treated with no drug, 1 μ M lapatinib, 100 nM dinaciclib, their combination and the combination of 1 μ M lapatinib with 10 μ M A1210477 for 6 and 12 h, respectively. Whole-cell lysates were prepared, subjected to western blotting and probed for the indicated proteins. **B** Cells from SKBR3, BT-474, MDA-MB-453, and HCC-1419 *HER2*-amplified breast cancer cell lines were treated with no drug or 100 nM dinaciclib for 2 h, and levels of the abundance of *MCL-1* mRNA were analyzed by qPCR. Data are normalized to *ACTB*; $n = 3$; error bars indicate \pm SEM. **C** BT-474 and MDA-MB-453 cells were treated with increasing concentrations of lapatinib and 10 μ M A1210477 or with increasing concentrations of lapatinib and 100 nM dinaciclib for 24 and 72 h respectively, and the percentage of viable cells was determined. $n = 3$; error bars indicate \pm SD. **D** BT-474 and MDA-MB-453 cells were treated with no drug or the combination of 1 μ M lapatinib and 100 nM dinaciclib for 24 and 72 h, respectively and the percentage of annexin V/PI-positive cells was determined by FACS. $n = 3$; error bars indicate \pm SD ("No Rx": No drug). **E** MCL-1 complexes were immunoprecipitated from the indicated *HER2*-amplified breast cancer cell lines following 6 h (BT-474) and 12 h treatment (MDA-MB-453) with no drug, 1 μ M lapatinib, 100 nM dinaciclib, and their combination. An IgG-matched isotype antibody was served as an immunoprecipitation control. The interaction between MCL-1 and BIM EL/BAK proteins was investigated ("No Rx": No drug). For Fig. 1B–D two-tailed Student's *t* test was performed. *p* values were corrected for multiple testing using the Bonferroni method. Differences were considered statistically different if $p < 0.05$. A *p* value < 0.05 is indicated by *, $p < 0.01$ by **, $p < 0.001$ by ***, $p < 0.0001$ by ****.

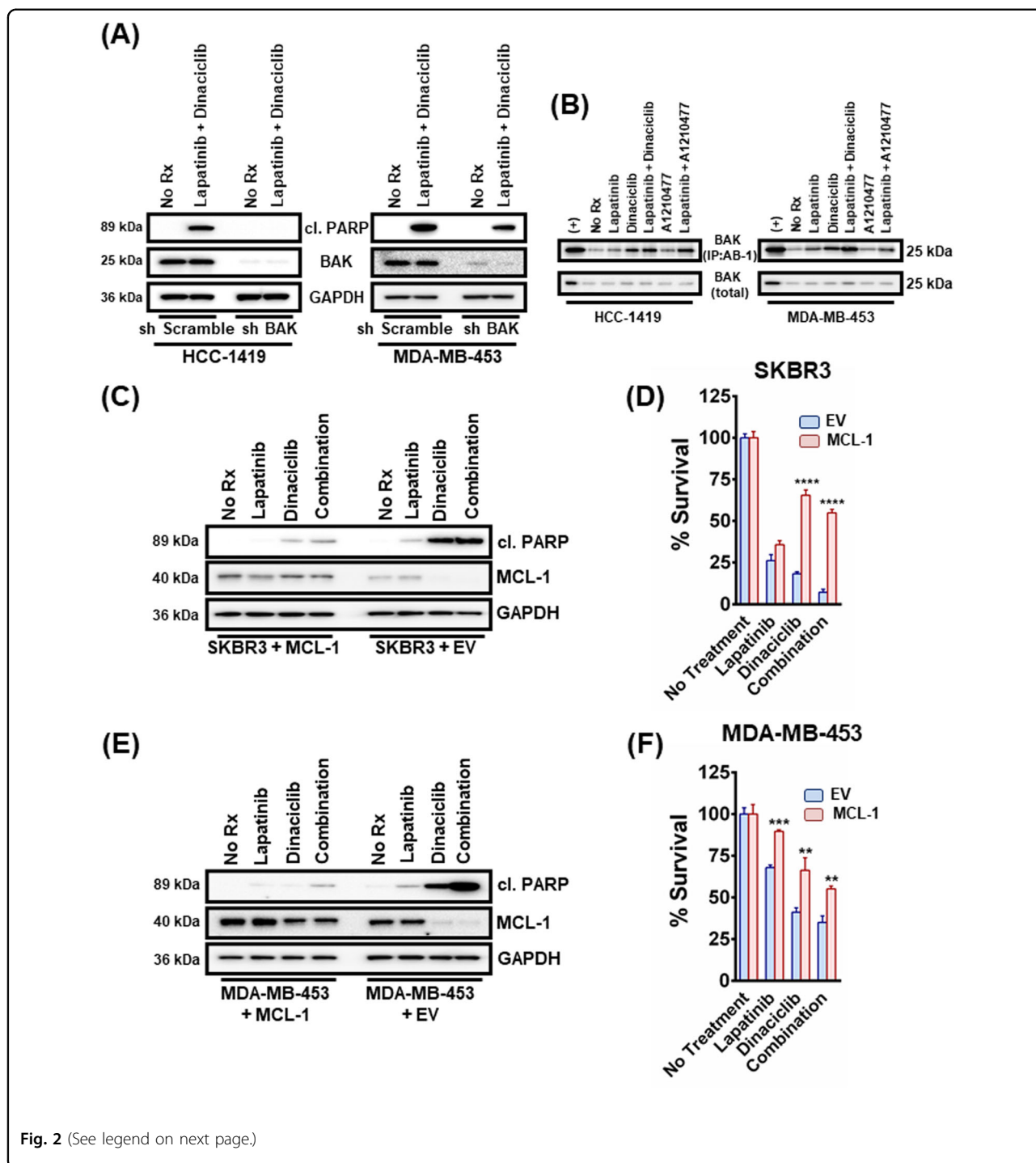


Fig. 2 (See legend on next page.)

the combination of dinaciclib and HER2 inhibition. Indeed, we found reduction of BAK by shRNA led to loss of apoptotic activity of the combination in two *HER2*-amplified HCC-1419 and MDA-MB-453 breast cancer cell lines where we were able to achieve sufficient knockdown (Fig. 2A). We next immunoprecipitated BAK with an antibody that exploits a conformation change in BAK

upon its activation and only recognizes this active BAK species²⁴. Consistent with an important role of MCL-1: BAK in combination toxicity, BAK was activated following either dinaciclib or A1210477 exposure, which was exacerbated upon the addition of lapatinib in both cases (Fig. 2B). Consistent with the enhanced apoptotic activity of the dinaciclib/lapatinib combination (Fig. 1A, B), BAK

(see figure on previous page)

Fig. 2 BAK is required for dinaciclib-induced cell death in *HER2*-amplified breast cancer cells and dinaciclib functions mainly by inhibiting MCL-1. **A** HCC-1419 and MDA-MB-453 cells were transduced with lentiviruses containing plasmids with an shRNA sequence targeting BAK or a non-targeting control. Puromycin-resistant cells were pooled after each infection. Cells were then treated with no drug, 1 μ M lapatinib, 100 nM dinaciclib or their combination overnight. Cell lysates were prepared and subjected to western blotting and probed for cleaved PARP, BAK, and GAPDH ("No Rx": No drug). **B** HCC-1419 and MDA-MB-453 cells were treated with no drug, 1 μ M lapatinib, 100 nM dinaciclib, 10 μ M A1210477 and their combinations (lapatinib/dinaciclib and lapatinib/A1210477) overnight and CHAPS lysates (using the zwitterionic detergent CHAPS, that can solubilize cells without promoting significant conformational changes in BAX and BAK, including the N-terminal Bak epitope exposure recognized by antibody Ab-1) were prepared and subjected to AB-1 IP and western blotting. Total cell lysates were analyzed in parallel. **C** SKBR3 control or MCL-1-expressing cells were treated with 1 μ M lapatinib, 100 nM dinaciclib, and their combination for 12 h. Whole-cell lysates were prepared, subjected to western blotting and probed for the indicated proteins. **D** SKBR3 control or MCL-1-expressing cells were treated with 1 μ M lapatinib, 100 nM dinaciclib, and their combination for 12 h and subjected to CellTiter-Glo. $n = 3$; error bars indicate \pm SD. **E** MDA-MB-453 control or MCL-1-expressing cells were treated with 1 μ M lapatinib, 100 nM dinaciclib, and their combination for 12 h. Whole-cell lysates were prepared, subjected to western blotting and probed for the indicated proteins. **F** MDA-MB-453 control or MCL-1-expressing cells were treated with 1 μ M lapatinib, 100 nM dinaciclib and their combination for 72 h and subjected to CellTiter-Glo. $n = 3$; error bars indicate \pm SD. For Fig. 2D, F two-tailed Student's t test was performed. p values were corrected for multiple testing using the Bonferroni method. Differences were considered statistically different if $p < 0.05$. A p value < 0.05 is indicated by *, $p < 0.01$ by **, $p < 0.001$ by ***, and $p < 0.0001$ by ****. EV: empty vector, (+): positive control, CHAPS: 3-((3-cholamidopropyl) dimethylammonio)-1-propanesulfonic acid.

was more active following dinaciclib/lapatinib than A1210477/lapatinib therapy (Fig. 2B).

While these data demonstrated a role of the MCL-1–BAK complex in dinaciclib/*HER2* inhibitor combination efficacy, we sought to investigate how important the MCL-1–BAK complex was to combination efficacy. For these experiments, in addition to the MDA-MB-453 cells, we used the SKBR3 *HER2*-amplified breast cancer cell line, which is very sensitive to MCL-1 inhibition^{4,25}. We found that the expression of exogenous MCL-1 was sufficient to mitigate the efficacy of both single-agent dinaciclib and the combination of dinaciclib and lapatinib to induce cell death (Fig. 2C), which translated into increased viability (Fig. 2D). In the MDA-MB-453 cells, rescue of MCL-1 expression was sufficient to block cell death (Fig. 2E) and increase total cell viability (Fig. 2F). To investigate if the other main pro-survival BCL2 proteins are implicated in dinaciclib-mediated apoptosis, we transiently overexpressed BCL2 and BCL-xL in the same two cell lines and treated with lapatinib, dinaciclib, and their combination (Supplementary Fig. 3 and Supplementary Fig. 4). Increased levels of BCL2 as well as BCL-xL did not result in significant suppression of the toxicity caused by the single agents or their combination, as determined by cleaved PARP expression (Supplementary Fig. 3A, C) or cell viability measurement (Supplementary Fig. 3B, D), demonstrating an MCL-1-specific effect caused by dinaciclib. However, while we did not see a sensitizing effect of the BCL-2 inhibitor venetoclax to lapatinib in the *HER2*-amplified breast cancer cell lines BT-474 or MDA-MB-453, we did see added toxicity with the tool BCL-xL inhibitor A-1331852, which was similar to that afforded by A-1210477 (Supplementary Fig. 4A, C). Similarly, A-1331852 sensitized the BT-474 and MDA-MB-453 cells to dinaciclib while venetoclax either did not (BT-474) or had a minimal effect (MDA-MB-453); strikingly, however,

A-1210477 had no sensitizing effect on dinaciclib, consistent with MCL-1 as the key dinaciclib target in *HER2*-amplified breast cancer (Supplementary Fig. 4B, D).

Dinaciclib sensitizes *HER2*-amplified breast cancer cells to the novel, selective *HER2* inhibitor tucatinib

As there are now at least seven FDA-approved *HER2* inhibitors²⁶, we wanted to corroborate our findings with some of the newer *HER2* inhibitors. Tucatinib is a novel, FDA-approved agent that has demonstrated more than 1000-fold selectivity for *HER2* over EGFR in in vitro assays²⁷ and significant efficacy in clinical trials for the treatment of metastatic *HER2*-positive breast cancer (NCT02614794)^{28–32}. As expected from a *HER2* inhibitor, tucatinib inhibited p-*HER2*, p-AKT and p-ERK in the *HER2*-amplified breast cancer cells BT-474 and MDA-MB-453¹⁷ (Fig. 3A). Addition of dinaciclib sensitizes the cancer cells to tucatinib as evidenced by increased cleaved PARP (Fig. 3A) and decreased cell viability in both cell lines (Fig. 3B, C), with their sensitivity reaching a plateau at about 1000 nM of tucatinib. To verify that complexes of MCL-1 with pro-apoptotic BCL2 proteins were disrupted by dinaciclib, we immunoprecipitated MCL-1 complexes in lysates derived from the MDA-MB-453 cells, following treatment with tucatinib, dinaciclib and their combination (Fig. 3D). Immunoprecipitation complex investigation confirmed that MCL-1:BAK complexes were disrupted following treatment with 100 nM dinaciclib (Fig. 3D).

Dinaciclib is effective in vivo at sensitizing *HER2*-amplified breast cancers to *HER2* inhibitors

We next determined whether the combination of dinaciclib and lapatinib would be effective in vivo. As mentioned, exposure time, at least in humans, is sufficiently different and prevents the ability of dinaciclib to potentially inhibit some CDK targets¹⁵. We found that

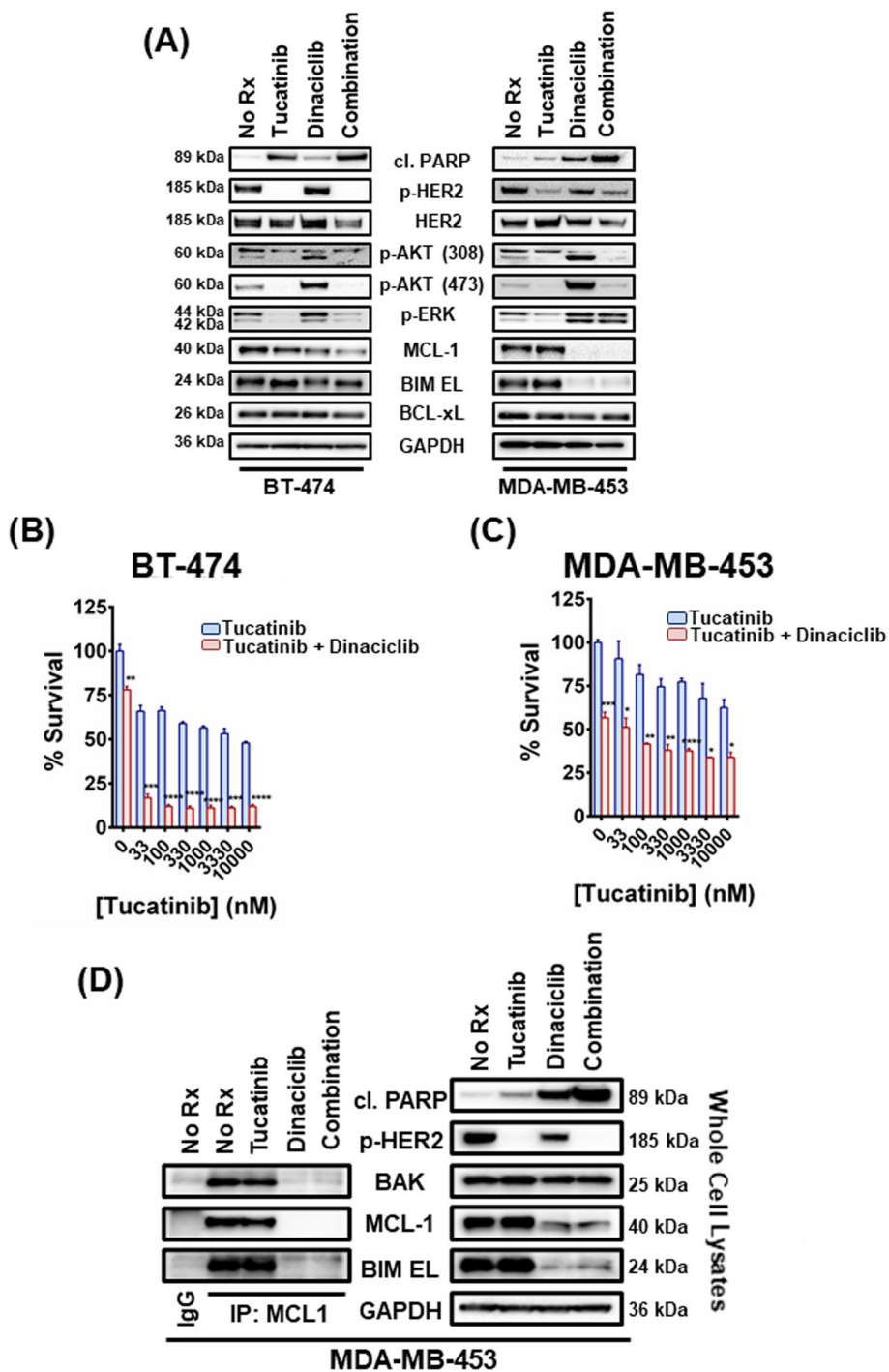
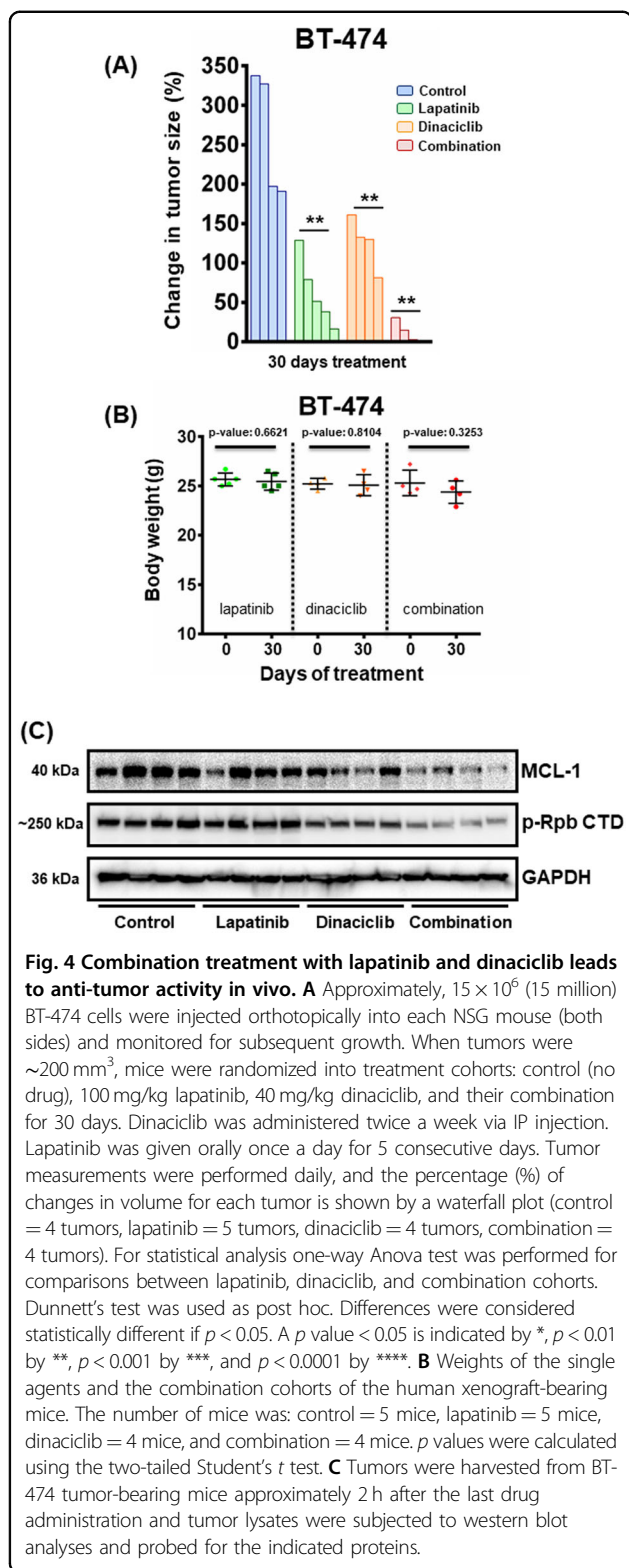


Fig. 3 Dinaciclib sensitizes *HER2*-amplified breast cancer cells to tucatinib and liberates BAK from MCL-1. **A** BT-474 and MDA-MB-453 cells were treated with no drug, 1 μ M tucatinib, 100 nM dinaciclib, and their combination for 6 and 12 h, respectively. Whole-cell lysates were prepared, subjected to western blotting and probed for the indicated proteins. **B** BT-474 cells were treated with increasing concentrations of tucatinib and 100 nM dinaciclib for 24 h and the percentage of viable cells was determined. $n = 3$; error bars indicate \pm SD. **C** MDA-MB-453 cells were treated with increasing concentrations of tucatinib and 100 nM dinaciclib for 48 h and the percentage of viable cells was determined. $n = 3$; error bars indicate \pm SD. **D** MCL-1 complexes were immunoprecipitated from MDA-MB-453 cells following 12 h treatment with no drug, 1 μ M tucatinib, 100 nM dinaciclib, and their combination. An IgG-matched isotype antibody was served as an immunoprecipitation control. The interaction between MCL-1 and BIM EL/BAK proteins was investigated. For Fig. 3B, C two-tailed Student's t test was performed; p values were corrected for multiple testing using the Bonferroni method. Differences were considered statistically different if $p < 0.05$. A p value < 0.05 is indicated by *, $p < 0.01$ by **, $p < 0.001$ by ***, and $p < 0.0001$ by ****. ("No Rx": No drug).



dinaciclib exhibited modest efficacy when administered alone but was sufficient to significantly sensitize BT-474 xenografts to lapatinib when dosed twice a week based on the clinical schedule (Fig. 4A and Supplementary Fig. 5A).

Mice remained healthy, based on their weight profiles, treated with the single agents or the combination (Fig. 4B). CDK9 phosphorylates the carboxy-terminal domain (CTD) of the RNA Polymerase II regulating elongation during transcription³³. Thus, CDK9 inhibitors regulate the expression of proteins with a short half-life, like MCL-1, and the reduction of the phosphorylation of the RNA polymerase II CTD at Ser2 may be used as a biomarker of the activity of CDK9 inhibitors³⁴. On-target inhibition of CDK9 was demonstrated by the suppression phosphorylation sites on the CTD of RNA polymerase II as well as MCL-1 following therapy with dinaciclib alone or in combination with lapatinib (Fig. 4C).

Dinaciclib sensitizes neratinib in HER2-amplified patient-derived xenograft (PDX) models

Neratinib is a potent irreversible pan-HER inhibitor, recently FDA-approved for HER2-amplified breast cancer². We tested neratinib in combination with dinaciclib in two HER2-amplified PDX models (WHIM 8 and WHIM 22)³⁵. While neratinib was effective at blocking the growth of the HER2-amplified tumors, the combination of dinaciclib and neratinib was superior to single-agent therapy in the WHIM 22 model (Fig. 5A and Supplementary Fig. 5B). In addition, there was no weight loss of the mice treated with the single agents or the combination, again suggesting tolerability (Fig. 5B). In the WHIM 8 model, we observed high activity of neratinib monotherapy; however, the combination of neratinib and dinaciclib resulted in uniformly robust tumor shrinkage ($>50\%$) (Fig. 5C and Supplementary Fig. 5C), with mice again not showing any significant weight loss (Fig. 5D). Cleaved PARP was elevated when the two drugs were administered together, indicating induction of apoptosis, while reduction of p-HER2 and MCL-1 advocates for the on-target effect of neratinib and dinaciclib, respectively (Fig. 5E). These data demonstrate potent combination efficacy of neratinib and dinaciclib in HER2-positive breast cancer PDX models.

Discussion

HER2 inhibitors administered in the neo-adjuvant setting increase progression-free survival (the time from treatment initiation until disease progression or worsening) and overall survival (the duration of patient survival from the time of treatment initiation) in HER2-amplified breast cancers^{36,37}. However, unlike similar RTK inhibitors in other solid tumor paradigms^{38–40} which have now replaced chemotherapy as standard of care, HER2 inhibitors are ineffective as monotherapy. Finding rational targeted therapy combinations with HER2 inhibitors therefore is likely the next step in order to find a therapeutic regimen that does not include chemotherapy.

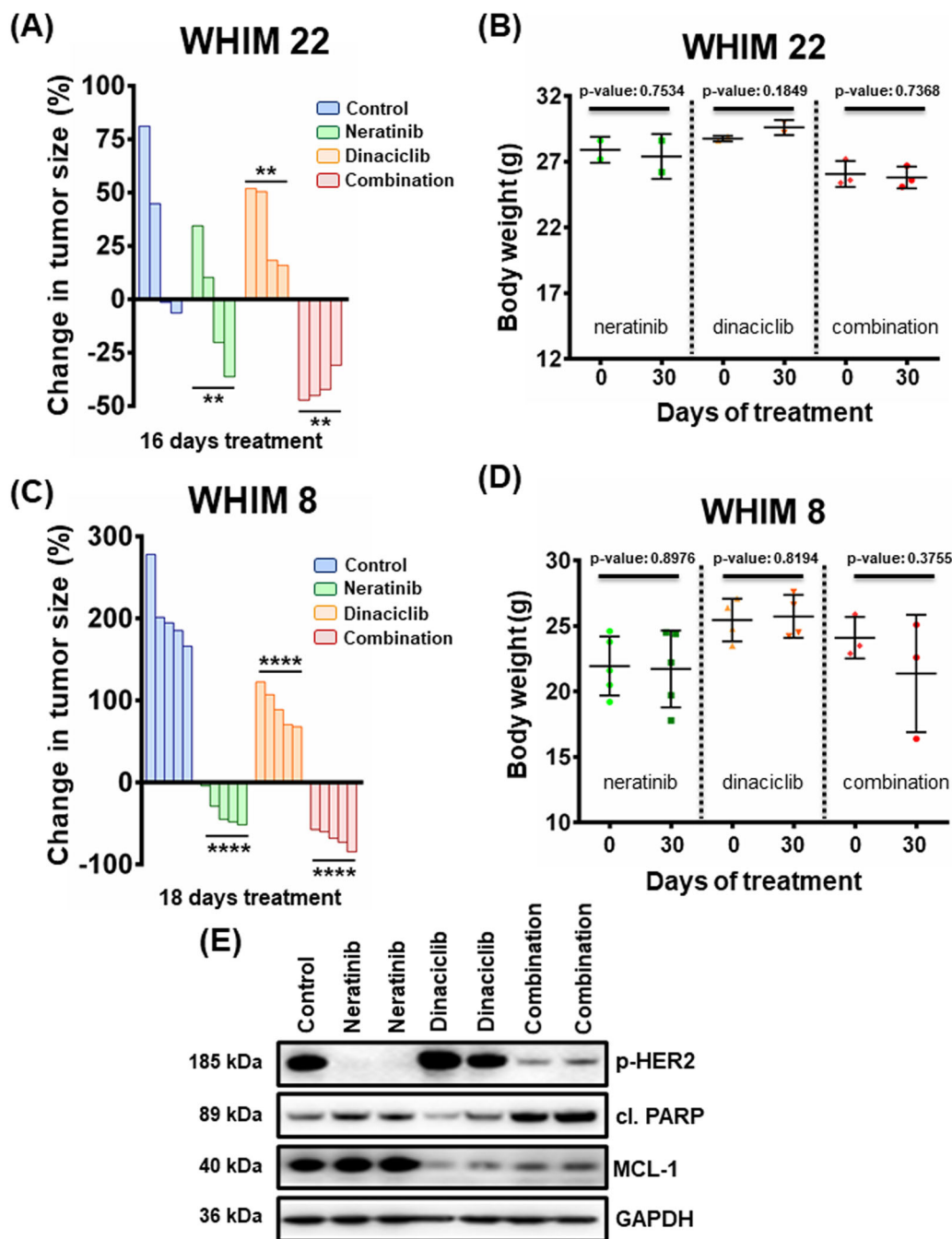


Fig. 5 Combination treatment with neratinib and dinaciclib leads to anti-tumor activity in vivo. **A** Approximately, 1.5×10^6 (1.5 million) cells derived from a *HER2*-positive breast cancer PDX model (WHIM 22) were injected orthotopically into each NSG mouse (both sides) and monitored for subsequent growth. After tumors reached a size of $\sim 150 \text{ mm}^3$, mice were treated with 40 mg/kg neratinib 5 days a week (Monday–Friday), 40 mg/kg dinaciclib twice a week, or their combination for 16 days. Tumor measurements were performed every day by calipers, and the percentage (%) of changes in volume for each tumor is shown by a waterfall plot (control = 4 tumors, neratinib = 4 tumors, dinaciclib = 4 tumors, combination = 4 tumors). For statistical analysis one-way Anova test was performed for comparisons between neratinib, dinaciclib, and combination cohorts. Dunnett’s test was used as post hoc. Differences were considered statistically different if $p < 0.05$. A p value < 0.05 is indicated by *, $p < 0.01$ by **, $p < 0.001$ by ***, and $p < 0.0001$ by ****. **B** Weights of the WHIM 22 PDX model-bearing mice of the single agents and the combination cohorts. The number of mice was: control = 2 mice, neratinib = 2 mice, dinaciclib = 2 mice, and combination = 3 mice. p Values were calculated using the two-tailed Student’s t test. **C** Same as **A** using the WHIM 8, *HER2*-positive breast cancer PDX model (18 days of treatment, control = 5 tumors, neratinib = 5 tumors, dinaciclib = 4 tumors, combination = 3 tumors). **D** Same as **B** using the WHIM 8 PDX model. The number of mice was: control = 5 mice, neratinib = 5 mice, dinaciclib = 2 mice, and combination = 3 mice. **E** Tumors were harvested from WHIM 8 PDX tumor-bearing mice approximately 2 h after the last drug administration and tumor lysates were subjected to western blot analyses and probed for the indicated proteins.

Indeed, chemotherapy has already begun to be de-emphasized in breast cancer, in particular hormone positive breast cancer⁴¹. The reason for de-escalation is the broad and lasting effects of chemotherapy-induced toxicity, which has been well described in breast cancer. Toxicities are numerous and cover a wide range of tissues. Cardiac toxicity, including congestive heart failure, is contributed by anthracyclines like doxorubicin⁴². Reproductive toxicity is very common for breast cancer undergoing adjuvant chemotherapy: for instance, in 280 young (aged 24–45) breast cancer patients, over 90% suffered from chemotherapy-related amenorrhea⁴³. While there remains controversy, a large Swedish study demonstrated women treated with chemotherapy for their breast cancer had higher risk pregnancies⁴⁴. Chemotherapy-induced bone loss is also a significant toxicity with considerable morbidity^{45,46}. In addition to overt tissue toxicity, chemotherapy delivered during breast cancer treatment increases the risk of secondary cancers, in particular acute myeloid leukemia^{47,48}.

Recently, we reported that levels of the endogenous MCL-1 inhibitor, NOXA, are uniformly depressed in *HER2*-amplified breast cancers, as a result of a co-amplified intronic microRNA that targets the estrogen receptor (ER), which in turn leads to loss of ER-driven *NOXA* transcription⁴. This can be overcome by the addition of MCL-1 BH3 mimetics, which Merino et al.⁵ also demonstrated. However, the toxicity of these drugs in clinical trials remains to be defined. Interestingly, we also found co-targeting BCL-xL with *HER2* is effective (Supplementary Fig. 4A, C), verifying results that have previously been reported²⁵. In Fig. 2 and Supplementary Fig. 3B, D, we provide evidence that dinaciclib and consequently its combination with lapatinib target mainly MCL-1. However, in SKBR3 cells overexpression of BCL-xL partially rescues sensitivity to dinaciclib and its combination with lapatinib (Supplementary Fig. 3B), albeit to a smaller extent than overexpression of MCL-1 does (Fig. 2D). This could be explained by the subsequent binding of the freed BAK to BCL-xL that is supplied exogenously, for which BAK has also affinity²³. While small molecule BCL-xL inhibitors have so far proven too toxic^{49,50}, other strategies to target BCL-xL, for instance, PROTACS, are being developed⁵¹. Indeed, Brugge and colleagues demonstrated potent preclinical *in vivo* activity of the dual BCL-xL/BCL-2 inhibitor navitoclax with the *HER2*-targeting antibody–drug conjugate trastuzumab emtansine⁵².

In contrast to the fairly unknown toxicity of MCL-1 inhibitors, dinaciclib is a CDK1, 2, 5, and 9 inhibitor that has demonstrated limited toxicities as a monotherapy, many of which were transient^{6,53}. CDK9 is part of the CAK complex, which is responsible for phosphorylating the C-terminus of RNA polymerase II, regulating

elongation during transcription³³. Although there are other cyclin-dependent kinases that are capable of phosphorylating the CTD of the RNA Polymerase II, like CDK7 and CDK8, the only one that activates gene expression in a catalytic manner is CDK9⁵⁴. CDK9 inhibitors regulate the expression of proteins with a short half-life. In this context dinaciclib has been reported to suppress the expression levels of the homologous recombination (HR) repair factors Rad51 and BRCA1 as well as c-Myc^{55,56}. Notwithstanding the fact that MCL-1 is not the only protein that is downregulated after treatment with dinaciclib, the lack of its pro-apoptotic partner, NOXA, in *HER2*-amplified breast cancers⁴ makes it likely the most important dinaciclib target in *HER2*-amplified breast cancers. Of note, there are other CDK inhibitors that have been explored for the treatment of *HER2*-amplified breast cancers, but no correlation with the expression of MCL-1 has been established⁵⁷.

Combining *HER2* inhibitors with a targeted therapy that can sensitize to apoptosis is an important therapeutic strategy since a robust apoptosis response is essential for mono-therapeutic targeted therapy in other RTK-driven cancers^{58–60}. In fact, in paradigms such as *EGFR*-mutant NSCLC, *EGFR* inhibition has limited success in patients whose cancers cannot undergo robust apoptosis^{58,61–65}. We believe the ability of dinaciclib to rationally combine with *HER2* inhibitors to induce apoptosis could therefore overcome the lack of efficacy *HER2* inhibitors in *HER2*-amplified breast cancers display, providing a targeted therapy combination strategy that could potentially eliminate the need for chemotherapy.

Since in addition to forming complexes with pro-apoptotic BCL-2 family members, MCL-1 also exerts oncogenic activity through other means^{66,67}, pharmaceutical reduction of MCL-1 expression may be more broadly effective than exposure to MCL-1 BH3 mimetics. Indeed, we noted increased sensitivity of dinaciclib and lapatinib compared to A-1210477 and lapatinib (Fig. 1). In addition, it should be noted that both lapatinib and neratinib are considered dual inhibitors of *HER2* and *EGFR*^{68,69}, which contributes to dermatologic and gastrointestinal adverse events^{70,71}. We also investigated the efficacy of the highly selective *HER2* inhibitor tucatinib combined with CDK9 inhibition. Consistently, our data support the notion that combination treatment of dinaciclib with selective *HER2* inhibition can be an effective therapy against *HER2*-amplified breast cancer.

In all, we propose that treating *HER2*-positive breast cancers by co-targeting *HER2* and MCL-1 can be achieved with the CDK inhibitor dinaciclib, which is clinically advanced. This combination may have advantages over MCL-1 BH3 mimetics, therefore maximizing the potential of *HER2* inhibitors to treat *HER2*-amplified breast cancers. Importantly, this offers a strategy that is

independent of chemotherapy, with the aim of improving responses and decreasing toxicity.

Materials and methods

Cell lines

The *HER2*-positive breast cancer cell lines used in this study were kindly provided by the Massachusetts General Hospital. SKBR3 cells were grown in DMEM/F12 medium with 10% fetal bovine serum (FBS) in the presence of 1 μ g/mL penicillin and streptomycin. BT-474 cells were cultured in DMEM medium containing 10% FBS, 1 μ g/ml penicillin, streptomycin, and 5 μ g/ml of insulin. MDA-MB-453, HCC-1419 were cultured in RPMI with 10% FBS in the presence of 1 μ g/mL penicillin and streptomycin. Cells were regularly screened for mycoplasma using a MycoAlert Mycoplasma Detection Kit (Lonza).

Reagents

The following drugs were purchased: Dinaciclib (SCH727965) for in vitro and in vivo studies (S2768; Selleckchem), lapatinib ditosylate (Tykerb) for in vitro and in vivo studies (M1802; Abmole), neratinib for in vivo studies (M1913; Abmole), A-1210477 (CT-A121; Chemietek), A-1331852 (22963; Cayman Chemicals), tucatinib (HY-16069; Medchem), and ABT-199 (venetoclax) (CT-A199; Chemietek). The antibodies used in this study were as follows: Anti-Bak (AB-1 clone for IP) (AM03; EMD Millipore), anti-Bak (3814S; Cell Signaling), anti-Bim (C34C5) (2933S; Cell Signaling), anti-BCL-xL (54H6) (2764S; Cell Signaling), anti-Bcl-2 (D55G8) (Human Specific) (4223S; Cell Signaling), anti-cleaved PARP (Asp214) (D64E10) (5625S; Cell Signaling), anti-GAPDH (6C5) (sc-32233; Santa Cruz), anti-MCL-1 (S-19) (sc-819; Santa Cruz), anti-phospho-p44/42 MAPK (Erk1/2) (Thr202/Tyr204) (D13.14.4E) (4370S; Cell Signaling), anti-phospho-S6 Ribosomal Protein (Ser240/244) (D68F8) (5364S; Cell Signaling), anti-phospho-Akt (Thr308) (244F9) (4056S; Cell Signaling), anti-phospho-Akt (Ser473) (D9E) (4060S; Cell Signaling), anti-HER2/ErbB2 (29D8) (2165S; Cell Signaling), anti-phospho-HER2/ErbB2 (Tyr1248) (2247S; Cell Signaling), anti-phospho-Rpb1 CTD (Ser 2/5) (4375S; Cell Signaling), Normal Rabbit IgG for IP (sc-2027; Santa Cruz), and Normal Mouse IgG for IP (sc-2025; Santa Cruz).

Vector construction and establishing stable cell lines

For the short-hairpin RNA (shRNA) experiments, the lentiviral shRNA (shBAK) was purchased from Open Biosystems. shRNA designed against a scramble sequence (MISSION pLKO.1-shRNA control plasmid DNA) served as the control. The pLKO.1 puromycin-resistant vector backbone served as the basis for cell selection in puromycin following infection. Cells were transduced with plasmid containing viral particles that were generated in

293T cells and collected over 48 h. The human MCL1 expression vector was generated as previously described (2). The construct was transfected into 293T packaging cells along with the packaging plasmids and the lentivirus-containing supernatants were collected to transduce the cells.

Western blotting

Cell lines and tumors from BT-474 xenografts as well as PDXs were prepared and lysed in lysis buffer (20 mM Tris, 150 mM NaCl, 1% Nonidet P-40, 1 mM EDTA, 1 mM EGTA, 10% glycerol, and protease, and phosphatase inhibitors), incubated on ice for 15 min, and centrifuged at max speed for 10 min at 4 °C. Tumor lysates were homogenized with Tissuemiser (Fisher Scientific) in the lysis buffer described previously, incubated for 20 min on ice, and centrifuged at max speed for 10 min at 4 °C. Equal amounts of the detergent-soluble lysates were resolved using the NuPAGE Novex Midi Gel system on 4–12% Bis–Tris gels (Invitrogen), transferred to polyvinylidene fluoride membranes (PerkinElmer) in between six pieces of Whatman paper (Fisher Scientific) set in transfer buffer from Biorad with 20% methanol, and following transfer and blocking in 5% nonfat milk in PBS, probed overnight with the antibodies listed above. Representative blots from at least three independent experiments are shown in the figures. Chemiluminescence was detected with the Syngene G: Box camera (Synoptics).

Cell viability assay

For the Cell Titer-Glo experiments, 1000–3000 seeded cells per well in 96-well flat-bottom black plates were treated with 25 μ L of CellTiter-Glo (Promega), following continuous drug treatment (each time with the indicated drugs at the indicated concentrations), at 37° and 5% atmospheric CO₂ and immediately read on a Centro LB 960 microplate luminometer (Berthold Technologies) according to the Promega protocol. Quantification of no-treatment seeded cells was used to determine the total cell growth number over the experiment. All data are means \pm SD of three independent experiments ($n = 3$).

FACS apoptosis assay

Totally, 3×10^5 cells were seeded per well in six-well plates and drugged with 100 nM dinaciclib combined with 1 μ M lapatinib for 24 (BT-474) and 72 h (MDA-MB-453), or left untreated. Cells were incubated with propidium iodide and annexin V-Cy5 (BD Biosciences) together for 15 min and assayed on a Guava easyCyte 5 flow cytometer (Millipore Sigma). Analysis was performed using guava-Soft 3.1.1 software. Cells stained positive for annexin V and annexin V + propidium iodide were counted as apoptotic. All data are means \pm SD of three independent experiments ($n = 3$).

RNA extraction and qRT-PCR

RNA was isolated from cultured cells grown at sub-confluency using the Zymo Quick-RNA MiniPrep kit (Zymo Research), and RNA was reverse-transcribed to form cDNA molecules using cDNA synthesis kit superscript III (Invitrogen) on a 7500 Fast Real-Time PCR System (Life Technologies). The expression of *MCL-1*, and β -*ACTIN* (*ACTB*) was measured using a GENEAMP PCR System 9700 (Life Technologies) by measuring the fluorescence increases of SYBR Green (Roche). The primers for *MCL-1* forward 5'-GGGCAGGATTGTGACTC TCATT-3' and *MCL-1* reverse 5'-GATGCAGCTTTC TTGGTTTATGG-3' and for *ACTB* forward 5'-GGCAT GGGTCAGAAGGATT-3', and *ACTB* reverse 5'-AGGAT GCCTCTCTTGCTCTG-3'. To determine relative abundance of *MCL-1* in relation to *ACTB*, the Delta-Delta CT (cycle threshold) method was utilized. All data are means + SEM of three independent experiments ($n = 3$).

Immunoprecipitation

Cells were lysed in the same buffer above; 500 μ g of lysates were incubated each time with MCL-1 antibody (2000 ng), or rabbit IgG (2000 ng). Following the addition of 25 μ L of 1:1 PBS: prewashed Protein A Sepharose CL-4B beads (cat. no. 17-096303; GE Healthcare Life Sciences) to the antibody/lysate mix, samples were incubated with rotating motion overnight. Equal amounts of extracts (5% of immunoprecipitated protein) were also prepared. Representative blots from at least three independent experiments are shown in the figures. Chemiluminescence was detected with the Syngene G: Box camera (Synoptics).

BAK activation assay

Cells were treated as indicated and lysed in AB-1 amino terminal capture buffer (10 mM Hepes, 135 mM NaCl, 5 mM $MgCl_2$, 0.2 mM EDTA, 1% glycerol + 1% CHAPS, added fresh; pH 7.4); 1500 μ g of lysates for the assay were incubated each time with AB-1/BAK antibody (1000 ng). Following the addition of 25 μ L of 1:1 PBS: prewashed Protein A Sepharose CL-4B beads (cat. no. 17-0963-03; GE Healthcare Life Sciences) to the antibody/lysate mix, samples were incubated with rotating motion overnight. Equal amounts of extracts (2.5% of immunoprecipitated protein) were also prepared. Representative blots from at least three independent experiments are shown in the figures. Chemiluminescence was detected with the Syngene G: Box camera (Synoptics).

Xenograft studies

NSG female mice were injected with $\sim 15 \times 10^6$ BT-474 cells per 200 μ L of 1:1 (cells: Matrigel). Mice were injected intraductally both sides and monitored for tumor growth. When tumors reached ~ 200 mm³, the tumor-bearing mice were randomized to a no-treatment control group, a lapatinib group (100 mg/kg), a dinaciclib group (40 mg/

kg), or a combination group (same doses). Mice in the cohorts (control = 4 tumors, lapatinib = 5 tumors, dinaciclib = 4 tumors, combination = 4 tumors) were treated with dinaciclib via IP injection and 2 h later with lapatinib by oral gavage. The solvent for lapatinib was 1% Tween 80. Dinaciclib was formulated in 20% 2-hydroxy propyl- β -cyclo dextrin (Sigma-Aldrich). The tumors were measured daily by electronic caliper, in two dimensions (length and width), and with the formula $v = l \times (w)^2(\pi/6)$, where v is the tumor volume, l is the length, and w is the width (the smaller of the two measurements). The drug schedule was 5 days a week (Monday–Friday) for lapatinib and twice a week for dinaciclib for 30 days. For pharmacodynamic studies, tumors were harvested 2 h following the last lapatinib treatment, and tumors were snap frozen in liquid nitrogen. All mouse experiments were approved and performed in accordance with the Institutional Animal Care and Use Committee at VCU.

Patient-derived xenografts

Female NSG mice were inoculated with tumor pieces derived from two HER2 + breast cancer PDX models called WHIM 8 and WHIM 22 (Horizon Discovery Group³⁵, expanded as single cell suspensions and injected into experimental mice orthotopically at the amount indicated in the legend of Fig. 4. Tumor growth was monitored until tumors grew to treatable levels (~ 150 mm³). These mice were then randomized into four groups: control, neratinib (40 mg/kg), dinaciclib (40 mg/kg), and dinaciclib/neratinib combination treatment. The number of tumors per cohort was: control = 4 tumors, neratinib = 4 tumors, dinaciclib = 4 tumors, combination = 4 tumors for the WHIM 22 model and control = 5 tumors, neratinib = 5 tumors, dinaciclib = 5 tumors, combination = 5 tumors for the WHIM 8 model. Dinaciclib was formulated in 20% 2-hydroxy propyl- β -cyclo dextrin (Sigma-Aldrich), while the solvent for neratinib was 0.5% methocellulose—0.4% Tween 80. Mice in the cohorts were treated with dinaciclib via IP injection and 2 h later with neratinib by oral gavage. The drug schedule was 5 days a week (Monday–Friday) for neratinib and twice a week for dinaciclib for 16 days (WHIM 22) or 18 days (WHIM 8). For pharmacodynamic studies, tumors were harvested 2 h following the last neratinib treatment, and tumors were snap frozen in liquid nitrogen. Tumors were measured as per the BT-474 xenograft.

Statistical considerations

Two-tailed Student's t test was performed for Figs. 1B–D, 2D, F, 3B, D, Supplementary Fig. 1, Supplementary Fig. 3B, D, Supplementary Fig. 4 and Supplementary Fig. 5A–C using GraphPad Prism. p values were corrected for multiple testing using Bonferroni method.

For Figs. 4A, 5A and 5C one-way Anova test was performed for comparisons between lapatinib/neratinib, dinaciclib and combination cohorts. Dunnett's test was used as post hoc. Differences were considered statistically different if $p < 0.05$. A p value < 0.05 is indicated by *, $p < 0.01$ by **, $p < 0.001$ by ***, and $p < 0.0001$ by ****.

Acknowledgements

Services and products in support of the research project were generated by the Virginia Commonwealth University Cancer Mouse Models Core Laboratory, supported, in part, with funding to the Massey Cancer Center from NIH-NCI Cancer Center Support Grant P30 CA016059.

Funding

This study was supported by the Department of Defense Breast Cancer Research Program, W81XWH-18-1-0561 (M.S. and A.C.F.) the Breast Cancer Research Foundation and the Mary Kay Foundation.

Author details

¹Department of Oral and Craniofacial Molecular Biology, Philips Institute for Oral Health Research, VCU School of Dentistry and Massey Cancer Center, Virginia Commonwealth University, Richmond, VA 23298, USA. ²Department of Pathology, Virginia Commonwealth University School of Medicine and Massey Cancer Center, Richmond, VA 23220, USA. ³Department of Biostatistics, Virginia Commonwealth University, Richmond, VA 23298, USA. ⁴Division of Hematology, Oncology and Palliative Care, Virginia Commonwealth University and Massey Cancer Center, Richmond, VA 23298, USA. ⁵AstraZeneca Pharmaceuticals, 35 Gatehouse Dr., Waltham, MA 02451, USA. ⁶Human Oncology & Pathogenesis Program (HOPP), Memorial Sloan Kettering Cancer Center, New York, NY 10065, USA. ⁷Department of Pathology, Memorial Sloan Kettering Cancer Center, New York, NY 10065, USA

Author contributions

K.V.F., M.S., and A.C.F. performed the study concept and design; K.V.F. and A.C.F. performed the development of methodology and writing, review, and revision of the paper; K.V.F., S.J., R.K., C.K.F., B.H., M.P., J.K., M.G.D., S.A.B., and A.C.F. provided the acquisition, analysis and interpretation of data, and statistical analysis; all authors read and approved the final paper.

Conflict of interest

In the past 2 years M.S. has received funds from Puma Biotechnology, AstraZeneca, Daiichi-Sankio, Immunomedics, Targimmune and Menarini Ricerche, and is a cofounder of Medendi.org and a full employee of AstraZeneca. A.F. has served as a scientific advisor for AbbVie, Inc.

Ethics statement

The current study did not require ethical approval.

Publisher's note

Springer Nature remains neutral with regard to jurisdictional claims in published maps and institutional affiliations.

Supplementary information The online version contains supplementary material available at <https://doi.org/10.1038/s41419-021-03457-6>.

Received: 11 April 2020 Revised: 23 December 2020 Accepted: 3 January 2021

Published online: 15 February 2021

References

- Gianni, L. et al. Neoadjuvant chemotherapy with trastuzumab followed by adjuvant trastuzumab versus neoadjuvant chemotherapy alone, in patients with HER2-positive locally advanced breast cancer (the NOAH trial): a randomised controlled superiority trial with a parallel HER2-negative cohort. *Lancet* **375**, 377–384 (2010).
- Chan, A. et al. Neratinib after trastuzumab-based adjuvant therapy in patients with HER2-positive breast cancer (ExteNET): a multicentre, randomised, double-blind, placebo-controlled, phase 3 trial. *Lancet Oncol.* **17**, 367–377 (2016).
- Lynch, T. J. et al. Novel agents in the treatment of lung cancer: Fourth Cambridge Conference. *Clin. Cancer Res.* **13**, s4583–s4588 (2007).
- Floros, K. V. et al. Coamplification of miR-4728 protects HER2-amplified breast cancers from targeted therapy. *Proc. Natl. Acad. Sci. USA* **115**, E2594–e2603 (2018).
- Merino, D. et al. Synergistic action of the MCL-1 inhibitor S63845 with current therapies in preclinical models of triple-negative and HER2-amplified breast cancer. *Sci. Transl. Med.* **9**, eaam7049 (2017).
- Thomas, D. et al. Targeting acute myeloid leukemia by dual inhibition of PI3K signaling and Cdk9-mediated Mcl-1 transcription. *Blood* **122**, 738–748 (2013).
- Hsieh, A. C. et al. Genetic dissection of the oncogenic mTOR pathway reveals druggable addiction to translational control via 4EBP-eIF4E. *Cancer Cell* **17**, 249–261 (2010).
- She, Q. B. et al. 4E-BP1 is a key effector of the oncogenic activation of the AKT and ERK signaling pathways that integrates their function in tumors. *Cancer Cell* **18**, 39–51 (2010).
- Fu, W. et al. The cyclin-dependent kinase inhibitor SCH 727965 (dinaciclib) induces the apoptosis of osteosarcoma cells. *Mol. Cancer Therap.* **10**, 1018–1027 (2011).
- Xu, J. et al. Inhibition of cyclin E1 sensitizes hepatocellular carcinoma cells to regorafenib by mcl-1 suppression. *Cell Commun. Signal.* **17**, 85 (2019).
- Gregory, G. P. et al. CDK9 inhibition by dinaciclib potently suppresses Mcl-1 to induce durable apoptotic responses in aggressive MYC-driven B-cell lymphoma in vivo. *Leukemia* **29**, 1437–1441 (2015).
- Jane, E. P. et al. Dinaciclib, a cyclin-dependent kinase inhibitor promotes proteasomal degradation of Mcl-1 and enhances ABT-737-mediated cell death in malignant human glioma cell lines. *J. Pharmacol. Exp. Therap.* **356**, 354–365 (2016).
- Li, L. et al. Synergistic induction of apoptosis in high-risk DLBCL by BCL2 inhibition with ABT-199 combined with pharmacologic loss of MCL1. *Leukemia* **29**, 1702–1712 (2015).
- Song, K. A. et al. Increased synthesis of MCL-1 protein underlies initial survival of EGFR-mutant lung cancer to EGFR inhibitors and provides a novel drug target. *Clin. Cancer Res.* **24**, 5658–5672 (2018).
- Gojo, I. et al. Clinical and laboratory studies of the novel cyclin-dependent kinase inhibitor dinaciclib (SCH 727965) in acute leukemias. *Cancer Chemother. Pharmacol.* **72**, 897–908 (2013).
- Mita, M. M. et al. Randomized phase II trial of the cyclin-dependent kinase inhibitor dinaciclib (MK-7965) versus capecitabine in patients with advanced breast cancer. *Clin. Breast Cancer* **14**, 169–176 (2014).
- Faber, A. C. et al. Differential induction of apoptosis in HER2 and EGFR addicted cancers following PI3K inhibition. *Proc. Natl. Acad. Sci. USA* **106**, 19503–19508 (2009).
- Zhou, J. et al. AMPK mediates a pro-survival autophagy downstream of PARP-1 activation in response to DNA alkylating agents. *FEBS Lett.* **587**, 170–177 (2013).
- Yao, M. et al. The research on lapatinib in autophagy, cell cycle arrest and epithelial to mesenchymal transition via Wnt/Erk/PI3K-AKT signaling pathway in human cutaneous squamous cell carcinoma. *J. Cancer* **8**, 220–226 (2017).
- Erlich, S. et al. Differential interactions between Beclin 1 and Bcl-2 family members. *Autophagy* **3**, 561–568 (2007).
- Huang, H., Shah, K., Bradbury, N. A., Li, C. & White, C. Mcl-1 promotes lung cancer cell migration by directly interacting with VDAC to increase mitochondrial Ca²⁺ uptake and reactive oxygen species generation. *Cell Death Dis.* **5**, e1482 (2014).
- Ham, J. et al. Exploitation of the apoptosis-primed state of MYCN-amplified neuroblastoma to develop a potent and specific targeted therapy combination. *Cancer cell* **29**, 159–172 (2016).
- Willis, S. N. et al. Proapoptotic Bak is sequestered by Mcl-1 and Bcl-xL, but not Bcl-2, until displaced by BH3-only proteins. *Genes Dev.* **19**, 1294–1305 (2005).
- Griffiths, G. J. et al. Cell damage-induced conformational changes of the proapoptotic protein Bak in vivo precede the onset of apoptosis. *J. Cell Biol.* **144**, 903–914 (1999).
- Xiao, Y. et al. MCL-1 is a key determinant of breast cancer cell survival: validation of MCL-1 dependency utilizing a highly selective small molecule inhibitor. *Mol. Cancer Therap.* **14**, 1837–1847 (2015).

26. Choong, G. M., Cullen, G. D. & O'Sullivan, C. C. Evolving standards of care and new challenges in the management of HER2-positive breast cancer. *CA Cancer J. Clin.* **70**, 355–374 (2020).
27. Kulukian, A. et al. Preclinical activity of HER2-selective tyrosine kinase inhibitor tucatinib as a single agent or in combination with trastuzumab or docetaxel in solid tumor models. *Mol. Cancer Therap.* **19**, 976–987 (2020).
28. Shah, M. et al. FDA approval summary: tucatinib for the treatment of patients with advanced or metastatic HER2-positive breast cancer. *Clin. Cancer Res.* (2020).
29. Tucatinib Is Active Against Brain Metastases in HER2(+) Breast Cancer. *Cancer Discov.* **10**, 1090 (2020).
30. Lin, N. U. et al. Intracranial efficacy and survival with tucatinib plus trastuzumab and capecitabine for previously treated HER2-positive breast cancer with brain metastases in the HER2CLIMB trial. *J. Clin. Oncol.* **38**, 2610–2619 (2020).
31. Murthy, R. K. et al. Tucatinib, Trastuzumab, and Capecitabine for HER2-Positive Metastatic Breast Cancer. *N. Engl. J. Med.* **382**, 597–609 (2020).
32. Tucatinib Impresses in Breast Cancer. *Cancer Discov.* **10**, 7 (2020).
33. Bieniasz, P. D., Grdina, T. A., Bogerd, H. P. & Cullen, B. R. Recruitment of cyclin T1/P-TEFb to an HIV type 1 long terminal repeat promoter proximal RNA target is both necessary and sufficient for full activation of transcription. *Proc. Natl. Acad. Sci. USA* **96**, 7791–7796 (1999).
34. Natori, A. et al. Mechanisms of action of a dual Cdc7/Cdk9 kinase inhibitor against quiescent and proliferating CLL cells. *Mol. Cancer Therap.* **10**, 1624–1634 (2011).
35. Li, S. et al. Endocrine-therapy-resistant ESR1 variants revealed by genomic characterization of breast-cancer-derived xenografts. *Cell Rep.* **4**, 1116–1130 (2013).
36. Slamon, D. J. et al. Use of chemotherapy plus a monoclonal antibody against HER2 for metastatic breast cancer that overexpresses HER2. *N. Engl. J. Med.* **344**, 783–792 (2001).
37. Piccart-Gebhart, M. J. et al. Trastuzumab after adjuvant chemotherapy in HER2-positive breast cancer. *N. Engl. J. Med.* **353**, 1659–1672 (2005).
38. Kwak, E. L. et al. Anaplastic lymphoma kinase inhibition in non-small-cell lung cancer. *N. Engl. J. Med.* **363**, 1693–1703 (2010).
39. Sequist, L. V. et al. First-line gefitinib in patients with advanced non-small-cell lung cancer harboring somatic EGFR mutations. *J. Clin. Oncol.* **26**, 2442–2449 (2008).
40. Chapman, P. B. et al. Improved survival with vemurafenib in melanoma with BRAF V600E mutation. *N. Engl. J. Med.* **364**, 2507–2516 (2011).
41. Sparano, J. A. et al. Adjuvant chemotherapy guided by a 21-gene expression assay in breast cancer. *N. Engl. J. Med.* **379**, 111–121 (2018).
42. Bird, B. R. & Swain, S. M. Cardiac toxicity in breast cancer survivors: review of potential cardiac problems. *Clin. Cancer Res.* **14**, 14–24 (2008).
43. Liem, G. S. et al. Chemotherapy-related amenorrhea and menopause in young Chinese breast cancer patients: analysis on incidence, risk factors and serum hormone profiles. *PLoS ONE* **10**, e0140842 (2015).
44. Dalberg, K., Eriksson, J. & Holmberg, L. Birth outcome in women with previously treated breast cancer—a population-based cohort study from Sweden. *PLoS Med.* **3**, e336 (2006).
45. Ghant, M. F. et al. Zoledronic acid prevents cancer treatment-induced bone loss in premenopausal women receiving adjuvant endocrine therapy for hormone-responsive breast cancer: a report from the Austrian Breast and Colorectal Cancer Study Group. *J. Clin. Oncol.* **25**, 820–828 (2007).
46. Brufsky, A. Management of cancer-treatment-induced bone loss in postmenopausal women undergoing adjuvant breast cancer therapy: a Z-FAST update. *Semin. Oncol.* **33**, S13–S17 (2006).
47. Rosenstock, A. S. et al. Acute myeloid leukemia and myelodysplastic syndrome after adjuvant chemotherapy: a population-based study among older breast cancer patients. *Cancer* **124**, 899–906 (2018).
48. Smith, R. E. et al. Acute myeloid leukemia and myelodysplastic syndrome after doxorubicin-cyclophosphamide adjuvant therapy for operable breast cancer: the National Surgical Adjuvant Breast and Bowel Project Experience. *J. Clin. Oncol.* **21**, 1195–1204 (2003).
49. Kaefer, A. et al. Mechanism-based pharmacokinetic/pharmacodynamic meta-analysis of navitoclax (ABT-263) induced thrombocytopenia. *Cancer Chemother. Pharmacol.* **74**, 593–602 (2014).
50. Mason, K. D. et al. Programmed anuclear cell death delimits platelet life span. *Cell* **128**, 1173–1186 (2007).
51. Khan, S. et al. A selective BCL-X(L) PROTAC degrader achieves safe and potent antitumor activity. *Nat. Med.* **25**, 1938–1947 (2019).
52. Zoeller, J. J. et al. Neutralization of BCL-2/X(L) enhances the cytotoxicity of T-DM1 in vivo. *Mol. Cancer Therap.* **18**, 1115–1126 (2019).
53. Kumar, S. K. et al. Dinaciclib, a novel CDK inhibitor, demonstrates encouraging single-agent activity in patients with relapsed multiple myeloma. *Blood* **125**, 443–448 (2015).
54. Napolitano, G., Majello, B., Licciardo, P., Giordano, A. & Lania, L. Transcriptional activity of positive transcription elongation factor b kinase in vivo requires the C-terminal domain of RNA polymerase II. *Gene* **254**, 139–145 (2000).
55. Carey, J. P. W. et al. Synthetic lethality of PARP inhibitors in combination with MYC blockade is independent of BRCA status in triple-negative breast cancer. *Cancer Res.* **78**, 742–757 (2018).
56. Alagpulinsa, D. A., Ayyadevara, S., Yaccoby, S. & Shmookler Reis, R. J. A cyclin-dependent kinase inhibitor, dinaciclib, impairs homologous recombination and sensitizes multiple myeloma cells to PARP inhibition. *Mol. Cancer Therap.* **15**, 241–250 (2016).
57. Sun, B. et al. Inhibition of the transcriptional kinase CDK7 overcomes therapeutic resistance in HER2-positive breast cancers. *Oncogene* **39**, 50–63 (2020).
58. Faber, A. C. et al. BIM expression in treatment-naïve cancers predicts responsiveness to kinase inhibitors. *Cancer Discov.* **1**, 352–365 (2011).
59. Roulston, A., Muller, W. J. & Shore, G. C. BIM, PUMA, and the achilles' heel of oncogene addiction. *Sci. Signal.* **6**, pe12 (2013).
60. Bean, G. R. et al. PUMA and BIM are required for oncogene inactivation-induced apoptosis. *Sci. Signal.* **6**, ra20 (2013).
61. Wu, S. G., Liu, Y. N., Yu, C. J., Yang, P. C. & Shih, J. Y. Association of BIM deletion polymorphism with intrinsic resistance to EGFR tyrosine kinase inhibitors in patients with lung adenocarcinoma. *JAMA Oncol.* **2**, 826–828 (2016).
62. Huang, W. F. et al. BIM gene polymorphism lowers the efficacy of EGFR-TKIs in advanced non-small cell lung cancer with sensitive EGFR mutations: a systematic review and meta-analysis. *Medicines* **94**, e1263 (2015).
63. Su, W. et al. BIM deletion polymorphism predicts poor response to EGFR-TKIs in non-small cell lung cancer: an updated meta-analysis. *Medicines* **98**, e14568 (2019).
64. Cardona, A. F. et al. BIM deletion polymorphisms in Hispanic patients with non-small cell lung cancer carriers of EGFR mutations. *Oncotarget* **7**, 68933–68942 (2016).
65. Karachaliou, N. et al. BIM and mTOR expression levels predict outcome to erlotinib in EGFR-mutant non-small-cell lung cancer. *Sci. Rep.* **5**, 17499 (2015).
66. Morciano, G. et al. Mcl-1 involvement in mitochondrial dynamics is associated with apoptotic cell death. *Mol. Biol. Cell* **27**, 20–34 (2016).
67. Lee, K. M. et al. MYC and MCL1 cooperatively promote chemotherapy-resistant breast cancer stem cells via regulation of mitochondrial oxidative phosphorylation. *Cell Metab.* **26**, 633–647 e637 (2017).
68. Rabindran, S. K. et al. Antitumor activity of HKI-272, an orally active, irreversible inhibitor of the HER-2 tyrosine kinase. *Cancer Res.* **64**, 3958–3965 (2004).
69. Rusnak, D. W. et al. The effects of the novel, reversible epidermal growth factor receptor/ErbB-2 tyrosine kinase inhibitor, GW2016, on the growth of human normal and tumor-derived cell lines in vitro and in vivo. *Mol. Cancer Therap.* **1**, 85–94 (2001).
70. Frankel, C. & Palmieri, F. M. Lapatinib side-effect management. *Clin. J. Oncol. Nurs.* **14**, 223–233 (2010).
71. Sodergren, S. C. et al. Systematic review of the side effects associated with anti-HER2-targeted therapies used in the treatment of breast cancer, on behalf of the EORTC quality of life group. *Target. Oncol.* **11**, 277–292 (2016).